Sustainable Cities and Society 114 (2024) 105745

Contents lists available at ScienceDirect

Sustainable Cities and Society

journal homepage: www.elsevier.com/locate/scs

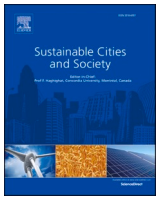

City configurations to optimise pedestrian level ventilation and wind comfort

Hakan Baş [a,*], Thomas Andrianne [b], Sigrid Reiter [c]

[a] Department of Architecture, Faculty of Engineering and Architecture, Izmir Katip Celebi University, Balatçık, Çiğli, Izmir 35620, Turkiye
[b] Fluid-Structure Interactions, Experimental Aerodynamics, University of Liege, Allée de la Découverte 9 (Bât. B52), Liège 4000, Belgium
[c] LEMA – Local Environment Management and Analysis, Urban and Environmental Engineering Department, University of Liege, Allée de la Découverte 9 (Bât. B52), Liège 4000, Belgium

ARTICLE INFO

Keywords:
City configuration
Pedestrian wind comfort
Outdoor ventilation
Computational fluid dynamics (CFD)
Wind tunnel

ABSTRACT

Mediterranean coastal cities encounter two conflicting urban environmental challenges. First, strong winds that pose a risk of pedestrian wind discomfort on coastal streets, and second, weak winds that lead to inadequate outdoor ventilation in inner urban fragments. This study aims to optimise pedestrian level ventilation and wind comfort in Izmir, a compact coastal city in the Mediterranean climate. Three hypothetical city configurations were created based on four morphological parameters: street layout, urban street canyon form, tower layout, and tower height variation. Computational fluid dynamics simulations of the city configurations were performed and validated by wind tunnel experiments. The weak, comfortable, and strong winds were determined and mapped at the pedestrian level to assess each city configuration's performance. The results show that using the strategy of a shifted coastal street layout with adding towers on second-row blocks results in a 20 % reduction of the maximum wind velocity ratio on coastal streets compared to a grid street layout without towers. Moreover, positioning step-up towers on step-up city blocks and shifted towers on step-down city blocks can increase pedestrian-level ventilation efficiency by up to 73 %. The research methodology and findings can be transferred to other climates and urban environments and guide urban designers.

1. Introduction

The livability and comfort of cities are under threat due to the catastrophic consequences of poor air quality, epidemics, and the urban heat island (UHI) effects, the phenomenon of where dense urban areas are much warmer than nearby rural areas (Voogt, 2004; Zhang et al., 2017). Urban ventilation with wind can alleviate the impact of UHI (Allegrini et al., 2015; He et al., 2020), poor air quality (Chen et al., 2021), and epidemics (Coccia, 2020; Orosa et al., 2020). However, due to their closely packed organisation, today's compact cities reduce wind flow and deteriorate urban ventilation. Although compact city configurations positively affect the environmental and social sustainability of cities by improving the efficiency of services (Mouratidis, 2019), they are exposed to the most air pollution (Buccolieri et al., 2010) and the highest UHI intensity (Stewart & Oke, 2012). This contradiction reveals the need to improve ventilation in compact cities.

In the compact coastal cities of the Mediterranean, wind (i.e., sea breeze) plays an important role in reducing UHI and improving ventilation. However, wind can also generate uncomfortable conditions for pedestrians and cyclists when they are too fast or generate sudden gusts near tall buildings (Reiter, 2010). Mainly, heterogeneous urban areas comprising low-rise and high-rise buildings (Stathopoulos & Wu, 1995) and coastal urban areas exposed to sea breeze from the open sea (Bas et al., 2022; Johansson & Yahia, 2020) are at risk of pedestrian wind discomfort.

In the context of the discussion above, Mediterranean cities suffer from weak wind conditions in deep street canyons and strong wind conditions in coastal streets and near tall buildings. Therefore, cities in the Mediterranean area must take advantage of sea breezes to reduce the adverse effects of UHI, air pollution, and epidemics. However, ensuring pedestrian-level wind (PLW) comfort is equally important. Based on this argument, this study focuses on the planning of pedestrian-level wind environment (PLWE) in compact coastal cities of the Mediterranean by optimizing pedestrian-level ventilation efficiency (PLVE) and pedestrian-level wind comfort (PLWC).

This study was conducted in Cape Punta, a compact coastal district of

* Corresponding author.
E-mail address: hakan.bas@ikc.edu.tr (H. Baş).

https://doi.org/10.1016/j.scs.2024.105745
Received 20 February 2024; Received in revised form 11 August 2024; Accepted 12 August 2024
Available online 13 August 2024

İzmir, a Mediterranean city in western Turkiye. Due to its dense urbanisation, Cape Punta faces UHI effects, air pollution, and pedestrian wind discomfort risk. Although the coastal areas benefit from the sea breeze, the inner regions of Cape Punta suffer from weak wind conditions. Furthermore, the presence of large and tall buildings poses a risk of pedestrian wind discomfort in their surrounding areas. Therefore, future urban planning scenarios in the urban renewal process of Cape Punta need to be created with multi-performance objectives that focus on both PLV efficiency and PLW comfort.

1.1. Literature review on spatial morphological parameters

Studies investigating the effect of urban morphology on the wind environment can be classified as city-scale and local-scale. City-scale studies have primarily focused on *urban ventilation corridors* (UVC) which aim to increase the speed and penetration of surrounding wind into the city (Wang et al., 2022) to reduce air pollution and the UHI effect (Gu et al., 2020; Xie et al., 2020). A new method of UVC based on *circuit theory* principles was also proposed to mitigate the UHI effect (Guo et al., 2023). The method assumes that when an airflow encounters a building-shaped barrier and is forced to branch, the airflow is distributed according to the inverse ratio of the wind resistance of each branch. By using this method, the shapes of UVCs can be determined by reclassifying the flow (Xie et al., 2022). Furthermore, many existing studies have focused on benefiting sea breezes to mitigate the UHI effect. He et al. (2019) stated that the influence of *precinct ventilation performance* under sea breeze could significantly mitigate UHI in a compact, high-rise urban area on the coast of Sydney, Australia.

Local-scale studies address urban ventilation at building, street, and neighborhood levels. Many studies recommend wider streets (Tsang et al., 2012; Hu & Yoshie, 2013), lower compactness, and lower building heights (He et al., 2019) to improve ventilation. Hang et al. (2012) suggested using shorter building lengths and higher heights or longer building lengths and lower heights to improve ventilation. He et al. (2018) stated that reducing the densities of streets while increasing their widths can improve ventilation in compact cities. These findings emphasize the negative correlation between urban ventilation requirements and compactness at a local scale.

In local-scale studies, the street aspect ratio, H/W (height-to-width), is the basic parameter that affects ventilation efficiency inside the canyon. If the street aspect ratio is low, above-roof flow enters the street canyon (Baik & Kim, 1999). However, this is unrealistic in many cities and contradicts today's compact city approach. Therefore, different ventilation strategies are used in compact cities. For example, buildings taller than the surrounding buildings are widely used to improve PLV efficiency because they have the potential to take high-speed wind at high altitudes. In vernacular architecture, wind catchers, which are chimney-like architectural elements placed on building roofs, capture atmospheric air and direct it to the space below, enhancing natural ventilation in indoor and outdoor areas (Montazeri, 2011; Chohan & Awad, 2022). However, in compact cities, street canyons are deep and narrow; therefore, more effective wind catchers were developed. Chew et al. (2017) studied the effect of newly designed wind catchers positioned at the roof level in a street canyon whose aspect ratio is 1 to improve urban ventilation. They found that a wind catcher can increase pedestrian-level wind speed by 2.5 times.

The step-up street canyon is another strategy to improve air circulation in compact cities (Ng, 2009; Chew et al., 2017). In a step-up canyon, the building heights gradually decrease toward the incoming wind, thus helping the buildings to ventilate the street canyon in front of them. Gu et al. (2011) confirmed that the uneven height of street canyons enhances pollutant dispersions. However, "step-down" canyons cause higher air pollution levels relative to the "even" and "step-up" canyons (Xie, 2005; Huang et al., 2009; Pan & Ji, 2024).

Step-up canyons and wind towers can increase outdoor ventilation (Ng, 2009; Xu et al., 2023) and pollutant dispersion (Hang et al., 2015; Chen et al., 2017), yet this can also lead to the *downwash effect*, which directs the high-speed wind from a higher altitude to the ground level due to the vertical pressure difference around a tower (Stathopoulos, 2009). Stathopoulos and Wu (1995) studied the wind flow interaction between tall and low-rise buildings. They found that the wind speed ratio between two buildings of different heights increases as the height of one of the buildings increases. The step-up canyon can meet cities' ventilation requirements if extra precautions are taken for pedestrian wind discomfort risk.

Many existing studies highlight the conflict between today's compact city approach and PLV efficiency and the motivation to improve urban ventilation with new techniques at the city scale and local scale without neglecting pedestrian wind comfort.

1.2. State of the art and innovation objectives

Based on the discussion in the literature review, this study differs from previous studies for three reasons. First, most studies focus on the effect of one building/urban morphological parameter on the PLW environment or separate PLV efficiency and PLW comfort issues with a single-purpose approach. However, none of them considered the design of the city configurations based on the cumulative effect of a set of strategies to improve PLV efficiency and PLW comfort in the context of the future design of a complex urban area simultaneously. Second, this study develops ventilation strategies in step-down canyons that cause most of the wind to pass over the buildings without entering the streets. Third, this study proposes a practicable evaluation method for spatially-averaged PLV efficiency and spatially-averaged PLW comfort based on climate-based target wind speed thresholds on a neighbourhood scale. In this respect, three city configurations were created based on a set of urban design strategies, and their PLV efficiency and PLW comfort were tested under specific site conditions.

The structure of the study is as follows. Section 2 presents the methodology, including the description of the city configurations, the experimental setup, and the validation of the numerical model with wind-tunnel measurements. Section 3 presents the results. Section 4 discusses the main findings considering other similar studies, and Section 5 presents the conclusions.

2. Methodology

This study proposes a design optimisation method that investigates the effect of various urban design strategies on the PLW environment. The method is presented in a step-by-step flowchart, as depicted in Fig. 1. The proposed method consists of two main complementary stages: determining the design strategies and city configurations and their performance evaluation. Computational fluid dynamics (CFD) simulations were performed to evaluate the performance of city configurations. CFD can effectively address different aspects of urban studies due to its flexibility (Shirzadi et al., 2020) and provide access to important quantities such as 3D velocities, pressure, and temperature throughout the domain of interest due to its important spatial resolution. CFD results were also validated by wind tunnel experiments performed at the Wind Tunnel Laboratory of the University of Liège (ULiège), Belgium.

2.1. Study area and climatic conditions

Izmir is located in the western part of Turkiye between 38.42°N and 27.14° E. The city lies in a typical Mediterranean climate with a hot-dry summer and wet/mild winter labelled with Csa according to the Köppen-Geiger climate classification. The average temperature is 10.7 °C in winter and 27.7 °C in summer (T.S.M.S, 2024). According to the wind data obtained from the closest meteorological station (200 m) to Cape Punta, the average speed of the local prevailing sea breeze is 2.9 m s^{-1} (z=2 m) (T.S.M.S, 2024). Sea breeze acts on the site from the

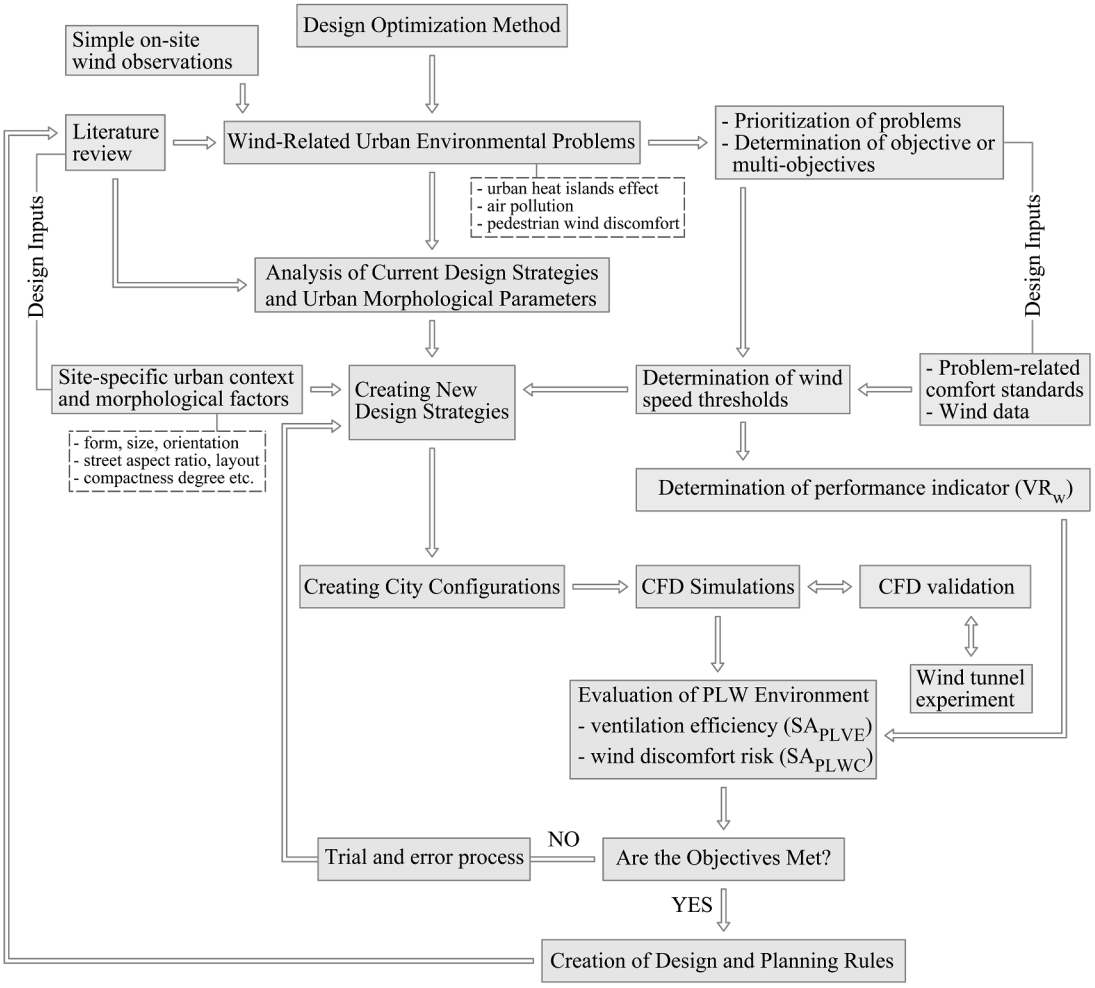

Fig. 1. Workflow and main steps of the design optimization method.

north-west. Especially in summer, its effect on the city's climate and air quality increases.

The Cape Punta was selected as the study area based on three specific criteria: a coastal district needing the most bioclimatic rehabilitation, a recreation centre with a wide range of pedestrian activities, and a compact city development consisting of buildings of various heights. Fig. 2 shows the Cape Punta surrounded by the sea on two sides (North and West).

Cape Punta's complex development history has created a diversified spatial morphology of its urban blocks. Urban development stages are divided into three construction periods: (i) low-rise (2–3 storeys) traditional row buildings; (ii) mid-rise (8–9 storeys) row and mid-rise

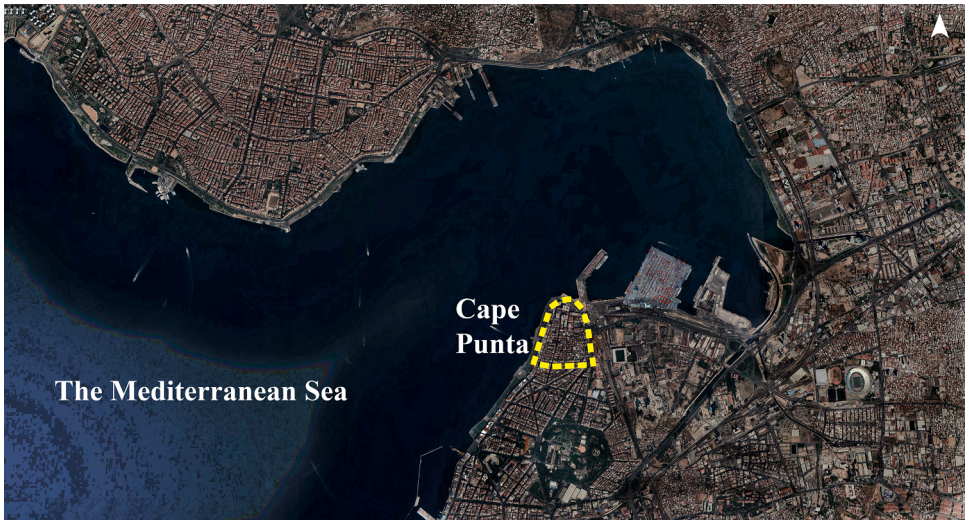

Fig. 2. Boundaries and plan view of Cape Punta in Izmir (adapted from Google Earth).

detached buildings; and (iii) high-rise buildings (20–25 storeys). The first characteristic building typology in the area is the low-rise, traditional Mediterranean buildings located along the coastline, which are important for city memory due to their historical context (Fig. 3b). However, after 1965, during rapid urbanization, most of them were replaced by mid-rise row and detached buildings (Fig. 3d, e) and thus lost their visual dominance. Mid-rise row buildings are not earthquake-resistant and need renewal. Furthermore, they prevent the incoming sea breeze from penetrating the deep street canyons (Arkon & Ozkol, 2014) and block the sea view of other buildings behind them. On the contrary, mid-rise detached buildings allow the flow of sea breeze but reduce the area's density (Fig. 3e).

The city's skyline has changed with the construction of the high-rise buildings (60 m) after the 2000s (Fig. 3c). Today, the high-rise buildings seem unbalanced since they are randomly positioned in the area. They improve ventilation but pose a significant risk of wind discomfort in their surroundings. Consequently, the overall spatial morphology of Cape Punta needs restructuring. All these issues were taken into account when creating city configurations.

2.2. Description of the design strategies and city configurations

In coastal cities, there are two wind flow regimes: frontal wind and top wind at the roof level. While coastal areas are open to the frontal and top wind, inner areas can receive only the top wind. In this regard, two design strategies gain importance: (1) to control the frontal wind in the coastal urban areas and around the influence areas of towers, and (2) to increase the penetration of the top wind into the inner urban areas. These strategies can minimize urban wind amplification and stagnation by meeting the common goal of filling the negative pressure areas behind the buildings with wind and reducing the pressure difference around the buildings. Therefore, urban morphological parameters should provide the *wind-directing effect,* which can direct wind to the leeward side of the buildings (negative pressure areas) in horizontal and vertical directions. Following this argument, *street layout, urban street canyon form, tower layo*ut, and *tower height variation* were determined as the four morphological parameters in forming city configurations.

Many factors were considered when determining the dimensions of the hypothetical urban template. First, the dimensions should be as small as possible to reduce the computational cost of CFD. Second, the maximum length should be 360 m to place the urban template on the WT turntable and conduct the experiments at 1/200 scale without causing wind blockage problems. Therefore, considering the dimensions of the buildings (60 m) and the streets (15 m), the maximum length of the urban template was determined to be 335 m. Finally, based on the approximate length-to-width ratio (1.4) of the Cape Punta and the dimensions of the buildings and the streets, the width of the urban template was determined to be 230 m. Thus, a hypothetical urban template of 335 m long and 230 m wide was created.

Based on the hypothetical urban template, three idealized city configurations (Conf. 1, Conf. 2, and Conf. 3) were created. The hypothetical and generic design approach was chosen to eliminate site-specific complications and gain greater control over the analysis (Oh, 2019). Design scenarios that shape the city configurations based on four

Fig. 3. View from Cape Punta and classification of existing building typologies: (a) panoramic west view of the heterogeneous urban skyline of Cape Punta (İzmirMag, 2016), (b) low-rise, traditional row buildings, (c) high-rise buildings, (d) mid-rise row buildings (e) mid-rise detached buildings.

morphological parameters are listed in Table 1.

Conf.1 is the *baseline configuration* comprising a cluster of 33 buildings in two regions (A and B). To be in harmony with the land shape of Cape Punta, rectangular-shaped buildings were used in the A region and curved-shaped buildings in the B region. The height of the buildings gradually rises from the first array (A1) to the fourth (A4) and decreases from the fourth array (A4) to the seventh (A7). Thus, a ridge-shaped urban skyline was created, integrating the step-up and step-down street canyons. Fig. 4a and c show the plan and perspective views of the city configurations, respectively, and Fig. 4b shows the front view of the city blocks.

The basic design scenario in Conf.1 is to keep the height of the coastal buildings (A1 and B1) smaller than the height of inner-city buildings. This strategy aims to protect the existing traditional low-rise row buildings on the coastline and to increase the wind catchment area of the street canyons at the roof level. It also aims to minimize the risk of PLW discomfort on the coastline, based on the argument that the smaller the building height, the lower the risk of wind discomfort (Reiter, 2010). However, a step-up canyon may pose a risk of PLW discomfort. The critical point is determining how much building façades will be directly exposed to wind flow. While a height difference between successive rows of blocks is too high, it may cause PLW discomfort risk; a low height difference may not adequately improve PLV efficiency. For this reason, the tested height difference between buildings was determined to be 6 m (two-storey).

Conf. 2 was created using Conf.1 as the *baseline configuration*. First, to reduce the PLW discomfort risk, a shifted coastal street layout was applied in the A1 and B1 arrays. This strategy aims to avoid direct exposure of the coastal streets to the frontal wind, thus reducing the wind speed (Bas et al., 2022). Second, towers were attached to the row block arrays (A3, A4, A5, and A6) to benefit from the top wind. The relative positions of the towers are crucial to increase the wind catchment potential of the city configuration. For this reason, row blocks are divided into three zones, and the towers are placed in three different positions, such as the blocks' left, middle, and right parts. The step-up tower layout was applied in A3 and A4 arrays, and a shifted tower layout in A5 and A6 rows. Thus, the towers were tried to be positioned in a way that would not screen the top wind. With the addition of the towers, the city configuration was transformed into a high-rise urban fabric that characterizes the future development of Cape Punta.

Conf. 3 was created by modifying the Conf. 2 with three changes. First, the height of the towers in rows A4 increased by 6 m more in Conf. 3. Second, new towers were attached to A2-B2 arrays, and the height of rows B3 increased by 18 m. This scenario aims to understand the effect of adding higher towers in the inner city and coastal streets on the PLW environment. Similar to Conf. 2, in Conf. 3, step-up tower layout in A2, A3, and A4 arrays, a shifted tower layout in A5 and A6 rows was provided.

The similarity of the three city configurations with the current Cape Punta was provided by using three characteristic building typologies in the area (low and mid-rise row buildings and high-rise buildings). Conf. 1 partially represents the area due to the absence of high-rise buildings. However, Conf. 2 and Conf. 3, although idealized, represent the complex, compact, and heterogeneous morphology of Cape Punta. They also propose a solution to the existing architectural and urban spatial problems in the area. In Conf. 2 and Conf. 3, the low-rise buildings on the coastline were revealed without obstructing the view of the rear part, and the high-rise buildings were distributed in a balanced manner in the area. Thus, a new approach to urban design was introduced without neglecting the morphological connection with the current urban area. Figs. 5 and 6 show the quantitative description of the morphological parameters used in creating city configurations.

Table 1
Design scenarios and strategies.

Conf. Name	Tower adding	Overall street layout	Coastal street layout
Conf. 1	–	grid	grid
Conf. 2	A3-A6 arrays	grid	shifted
Conf. 3	A2-A6, B2-B3 arrays	grid	shifted

The compactness degree of the city configurations was determined using three geometric indicators: the building height, the street aspect ratio (the ratio of mean height to width), and the building surface fraction (BSF=the ratio of building plan area to total plan area) based on the standardized, ''local climate zone'' (LCZ) classification system of Stewart and Oke (2012). The building height for the compact-midrise category in the LCZ classification is between 10 and 25 m, the street aspect ratio is 0.75–2, and the building surface fraction is 40–70 %. For the compact-highrise category, the building height is >25 m, the street aspect ratio is >2, and the building surface fraction is 40–60 %.

In the three-city configurations, building height and street aspect ratio increase from the configuration edges toward the interior. Conf. 1 demonstrates the characteristics of a compact-mid-rise settlement type with the heights of the row blocks between 12 and 30 m, the street aspect ratios between 0.8 and 2, and BSF of 49 %. With the adding towers to row blocks in Conf. 2 and Conf. 3, the building heights exceed 25 m, and the street aspect ratios reach 4.0 around the towers in Conf. 2 and 4.4 in Conf. 3. The compact-mid-rise settlement characteristics in the coastal part changed to the compact-high-rise settlement characteristics in the interior part of Conf. 2 and Conf. 3.

2.3. Determination of wind speed thresholds for climate-based design target

High wind speed is required for better outdoor ventilation, while low wind speed is desirable for pedestrian wind comfort. Therefore, it is necessary to determine the minimum and maximum *wind speed thresholds* to assess the PLV efficiency and PLW comfort at the pedestrian level simultaneously. While Ng (2009) proposed a breeze of 1.0 to 1.5 m s^{-1} to reduce thermal discomfort for a person in the shade when the temperature is 28 °C in a similar climate like İzmir, Xu and Xu (2020) recommend a wind speed of at least 1.0 m/s as a standard to enable outdoor air pollution diffusion. Considering heat stress and air pollution diffusion issues, we chose the minimum mean wind speed threshold as 1 m/s at the pedestrian level (z = 2 m). The maximum mean wind speed threshold was set at 3.6 m/s (Isyumon & Davenport, 1975), as Cape Punta is the central recreation zone of the city hosting walking and long-term seating places. Consequently, the targeted wind speed values for the wind environment optimisation are between 1.0 m s^{-1} and 3.6 m/s. Thus, a compromise between conflicting wind speed requirements was provided, which corresponds also to the thresholds chosen by Bas et al. (2022).

2.4. Evaluation indicator of PLV efficiency and PLW comfort

PLW comfort can mainly be evaluated by wind velocity and wind velocity ratio, while PLV efficiency can also be evaluated by various performance indicators such as the age of air, pollutant concentration, and purging flow rates (Zhao et al., 2020). In this study, wind velocity ratio (VR_W) is used as the performance indicator for three reasons. First, VR_W is a directly related indicator to this study's multi-objectives, including ventilation (He et al., 2019; Palusci et al., 2022), UHI (Ignatius et al., 2015; He et al., 2019), and pedestrian wind comfort (Baş et al., 2023). Second, VR_W can appropriately evaluate the ventilation conditions on a large scale, as it refers to the continuous flow of wind instead of on a point scale (Kato & Hiyama, 2012). Third, it is a practical performance indicator for evaluating the ventilation performance of large-scale urban areas.

VR_W is calculated by V/V_{ref} where V=mean wind velocity at the measuring point (z=2 m) and V_{ref}=inlet mean wind velocity (z=2 m). The targeted minimum and maximum design wind speed thresholds, which are 1.0 m/s and 3.6 m/s, correspond to VR_w=0.34 and VR_w=1.24,

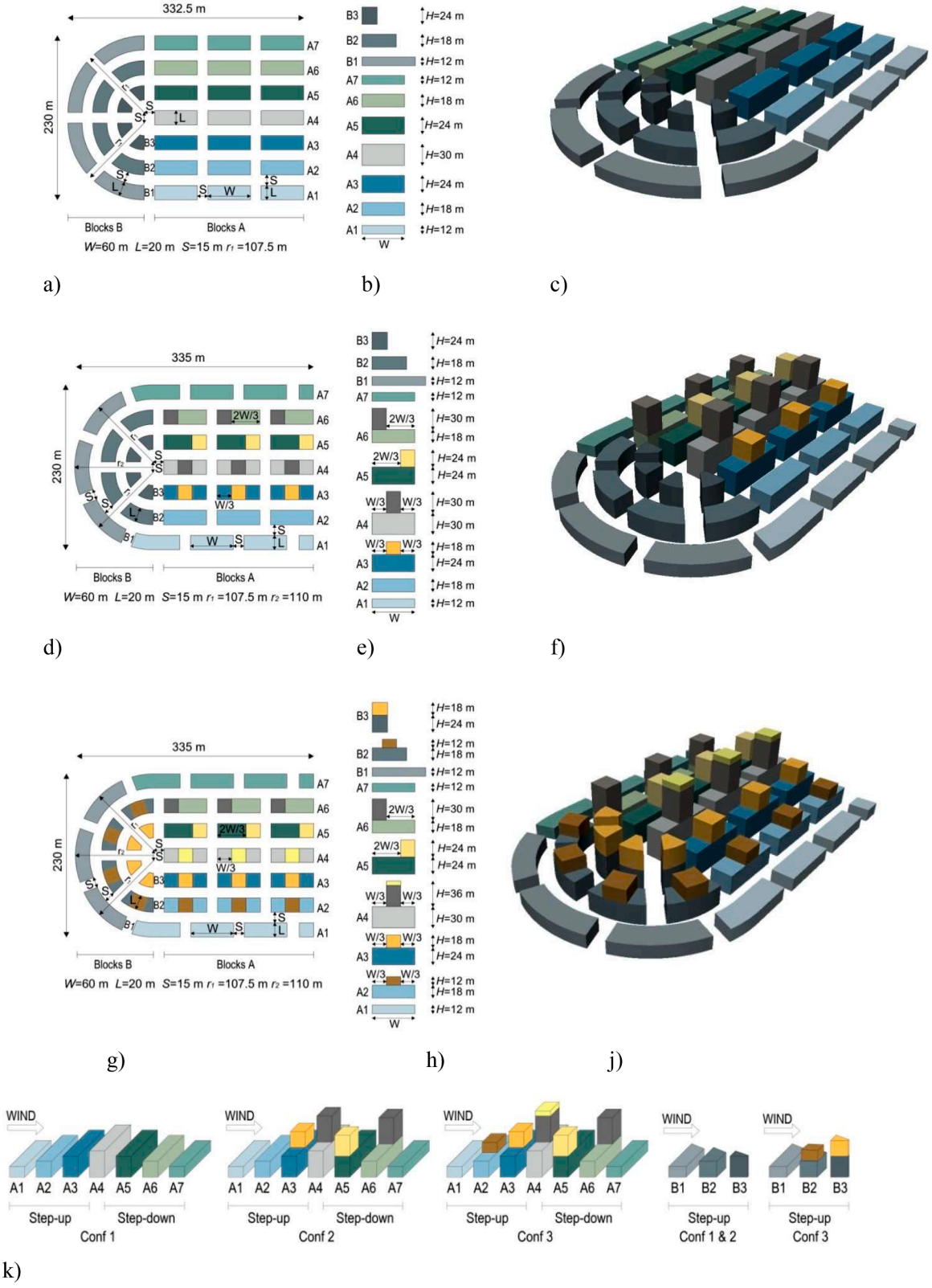

Fig. 4. Views of the city configuration design alternatives; (a) plan view of Conf. 1 (b) front view of Conf. 1 (c) perspective view of Conf. 1 (d) plan view of Conf. 2 (e) front view of Conf. 2 (f) perspective view of Conf. 2 (g) plan view of Conf. 3 (h) front view of Conf. 3 (j) perspective view of Conf. 3 (k) perspective views of city configurations (For A1–2, 'A' represents the block region; '1' represents the block position from bottom to top and '2' from right to left in the plan view).

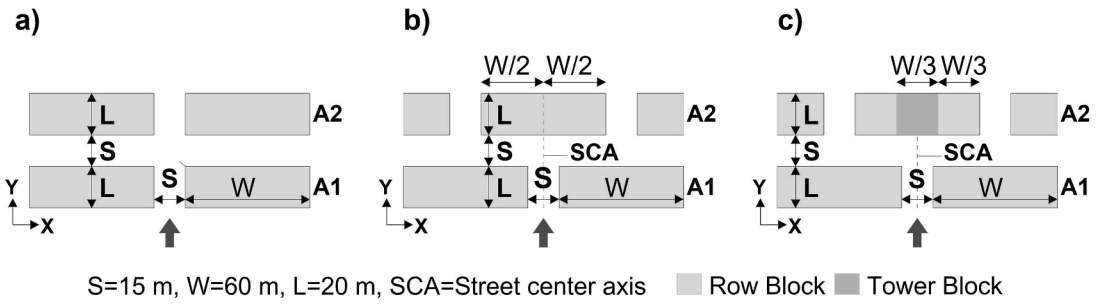

Fig. 5. Quantitative description of the street layout parameter (a) grid street layout (Conf. 1) (b) shifted street layout (Conf. 2) (c) shifted street layout and second-row block with a tower (Conf. 3).

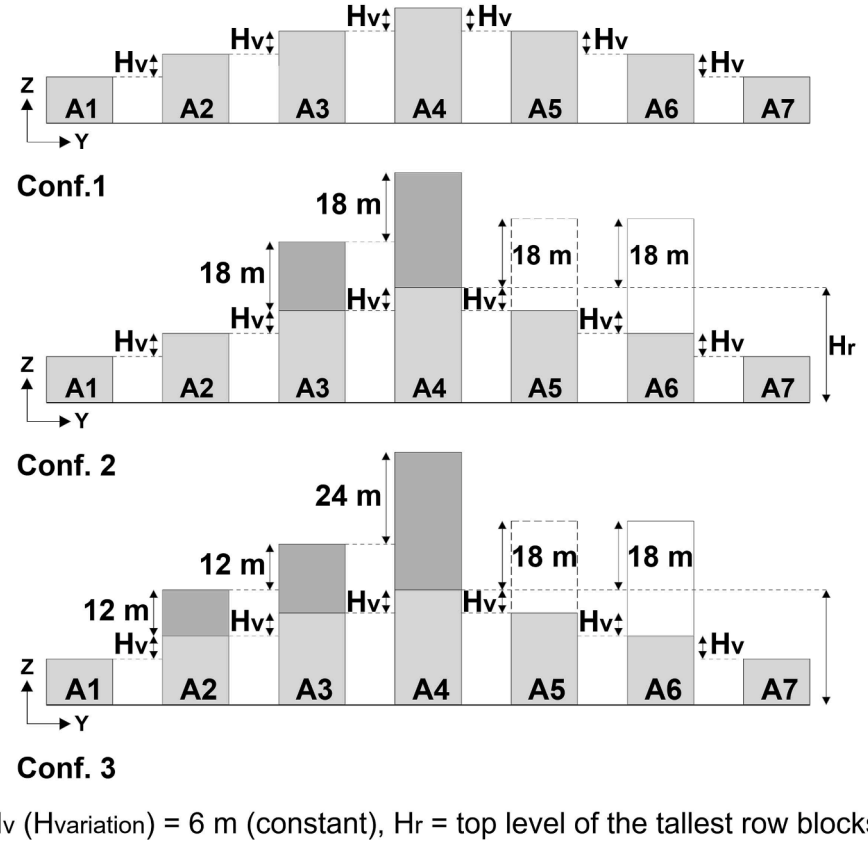

Fig. 6. Quantitative description of the urban street canyon parameter.

respectively. Three PLW velocity ratios are used to assess the PLW environment: (1) *weak* ($VR_w < 0.34$), (2) *strong* ($VR_w > 1.24$), and (3) *comfortable* $0.34 \leq VR_w \leq 1.24$. These thresholds are specific to the climate of Cape Punta and can be adjusted and redefined in other climates and sites.

Instead of calculating the VR_W only at specific measuring points, the spatially-averaged PLWE (SA_{PLWE}) of the city configurations was calculated. SA_{PLWE} refers to how much of the area meets the targeted wind speed thresholds in the whole wind flow evaluation domain. SA_{PLWE} of each city configuration was calculated using Eq. (1).

$$\text{SAPLWE}\ (\%) = \frac{\text{Area of wind flow domain}\ (0.34 \leq \text{VRw} \leq 1.24)}{\text{Area of whole wind flow assessment domain}\ (\text{VRw} \geq 0)} 100\% \quad (1)$$

Additionally, the following two equations were used to evaluate the spatially-averaged PLVE (SA_{PLVE}) and PLWC (SA_{PLWC}):

$$\text{SAPLVE}\ (\%) = \frac{\text{Area of wind flow domain (VRw } \geq 0.34)}{\text{Area of whole wind flow assessment domain (VRw } \geq 0)} 100\% \quad (2)$$

$$\text{SAPLWC}\ (\%) = \frac{\text{Area of wind flow domain (VRw } \leq 1.24)}{\text{Area of whole wind flow assessment domain (VRw } \geq 0)} 100\% \quad (3)$$

After calculating the SA_{PLWE}, the average SA_{PLWE} is calculated, including the results obtained under seven wind directions (0°, 15°, 30°, 45°, 60°, 75°, 90°). The design whose average SA_{PLWE} is the biggest will be considered the optimum design for both PLV efficiency and PLW comfort. Although the prevailing wind at the site is the sea breeze coming at an angle of 45°, the configurations were simulated under seven wind directions. Such an approach aims to develop transferable solutions to other parts of İzmir and other cities rather than performing site-specific wind planning only in Cape Punta.

2.5. Experimental setup

2.5.1. Measurement parameters of wind tunnel experiments

This section presents the validation of CFD through experiments conducted in the close circuit-type atmospheric boundary layer (ABL) of the wind tunnel (WT) of the University of Liège (ULiège) in Belgium. The use of both CFD and WT methods in this study is motivated by two reasons. Firstly, the test section of the WT has a width of 2.5 m and a height of 1.8 m; the fetch length is 15 m. Due to its long fetch length, it provides an ideal setup for creating accurate atmospheric boundary layer (ABL) conditions. Secondly, the published experimental data for CFD validation purposes in the literature represents simple city configurations rather than more complex city configurations consisting of curved geometries, shifted street layouts, and buildings in varied heights and arrangements used in this study. As such geometric differences can lead to differences in results, the same city model in both WT and CFD was used.

The buildings were produced from wooden blocks with laser-cut technology at a reduced geometric scale (λ_L=1:200) and Conf. 2 was installed on a 2 m diameter turntable in the wind tunnel test section, keeping the blockage ratio ($Area_{configuration}$ / $Area_{wind\ tunnel}$) is 2.7 %. Considering the exposure to the open sea at Cape Punta, the site was characterised by the surrounding terrain category 0′. The ABL wind profile (mean speed, turbulent content) for terrain category 0′ specified in Eurocode EN 1991–1-4 (1991) was produced in the test section of the wind tunnel using a barrier and an array of surface roughness blocks. The experimental setup, which includes the geometric model positioned on the turntable, measuring devices, and surface roughness blocks, is shown in Fig. 7a.

Conf. 2 was equipped with omnidirectional in-house Irwin probes developed at the Wind Tunnel Laboratory of ULiège on the basis of the

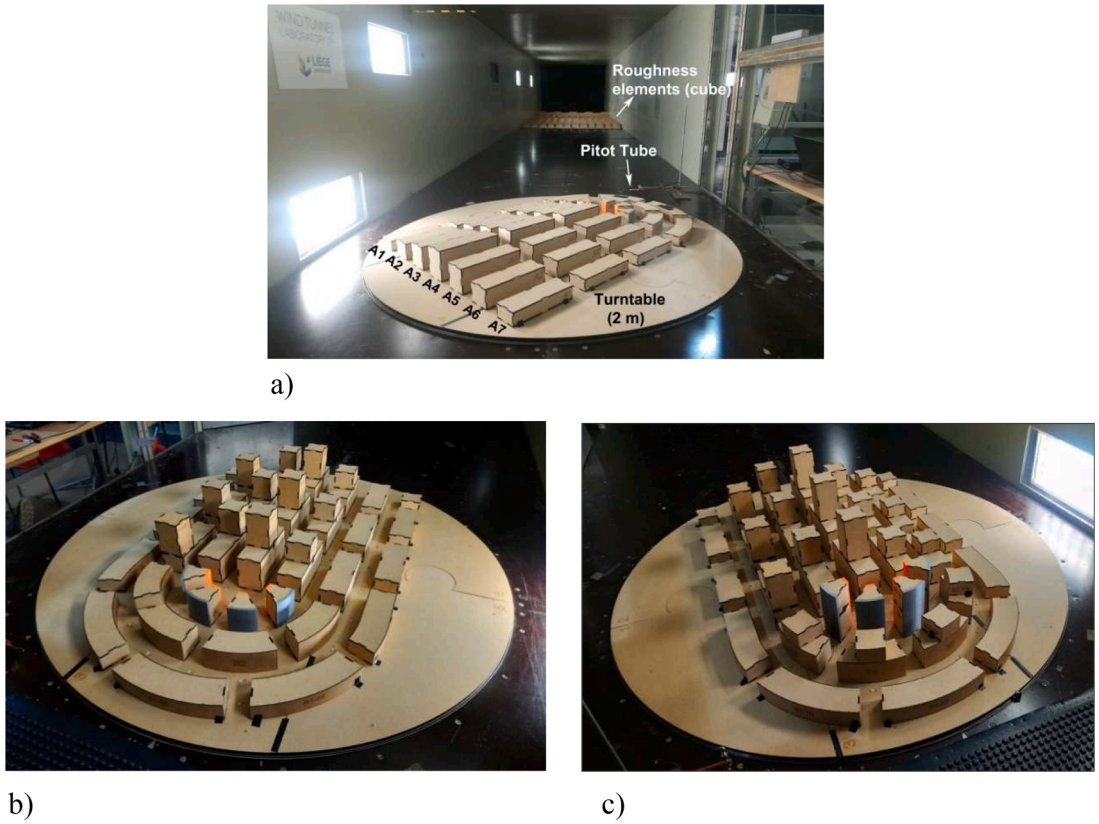

Fig. 7. Experimental setup in WT (a) setup for category 0′ (Conf. 1) (b) view of Conf. 2 (c) view of Conf. 3.

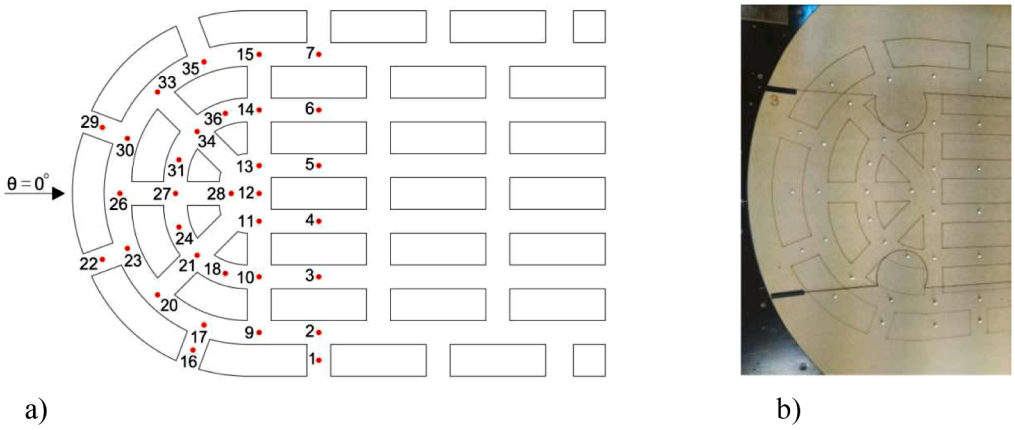

Fig. 8. (a) Measuring points map positioned in a plan view (Conf. 2) (b) produced measuring points (Irwin probe) map positioned on the turntable.

original work of Irwin (1981). Due to their straightforwardness, Irwin Probes can be installed in huge numbers on a model to predict mean wind speed and low-frequency speed fluctuations in PLW studies (Irwin, 1981). In particular, Irwin probes give access to the wind speed in the horizontal plane without information about the flow direction in this plane. It is nevertheless not necessary in the present case of ventilation and wind comfort evaluations. Due to their small size, their effect on wind flow is limited (Vita et al., 2020). The Irwin probes used have a velocity range between 1 m/s and 10 m/s with an accuracy of 1 % or the measured value. When determining the position of the measuring points, the potential locations of high and low-speed regions were considered. In total, 36 measurement points on the central axis of the streets at the pedestrian level were positioned. Fig. 8 displays the map of measuring points on Conf. 2 in plan view.

The equations specified in Eurocode EN (1991)-1–4 1991 were used in modelling the ABL wind profile. The mean wind speed at height z, $v_m(z)$ was specified using Eq. (1).

$$vm(z) = Cr(z).Co(z).vb \tag{1a}$$

where v_b is the basic wind speed, c_r (z) is the roughness factor, and $c_o(z)$ is the orography factor, taken as 1.0.

$$Cr(z). = kr\ .\frac{1}{\kappa}\ln\left(\frac{z}{zo}\right) \tag{2a}$$

where z_0 is the aerodynamic roughness length (z_0=0.003 for surrounding terrain category 0′) and k_r terrain factor depending on the roughness length z_0 calculated using:

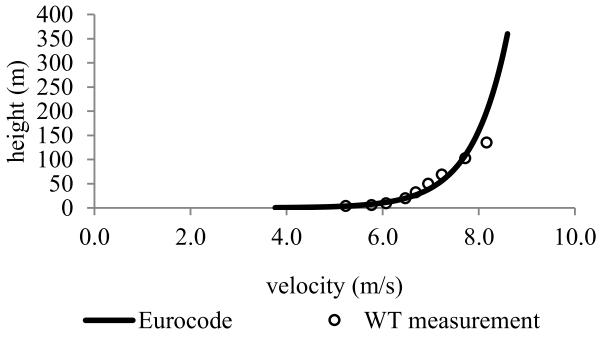

Fig. 9. The ABL vertical wind velocity profile measured in front of the empty turntable and Eurocode $V_m(z)$ profile for category 0′. (Dots represent WT measurements while lines represent formulas based on Eurocode EN (1991)-1-4 (1991)).

$$kr = 0.19.\left(\frac{zo}{zo,\ II}\right) \tag{3a}$$

where $z_{0,\ II}$ = 0,05 m (terrain category II)

The turbulent characteristics can be denoted by the turbulence intensity and the integral length scale of turbulence. The turbulence intensity $I_v(z)$ at height z was calculated using Eq. (4).

$$Iv\ (z) = \left(\frac{\sigma v}{vm(z)}\right) \tag{4}$$

The standard deviation of the turbulence σ_v was calculated using Eq. (5).

$$\sigma_v = k_r.v_b.k_I \tag{5}$$

where k_I is the turbulence factor taken as 1.0.

The turbulent length scale L(z) for heights z below 200 m was calculated using Eq. (6)

$$L(z) = Lt\ .\left(\frac{z}{zt}\right) \tag{6}$$

where a reference height of z_t = 200 m, a reference length scale of L_t = 300 m, and with $\alpha = 0{,}67 + 0{,}05\ \ln(z_0)$.

The ABL wind profile was correctly simulated in the empty test section up to 135 m, which is higher than the tallest building (66 m) in the configurations. Fig. 9 compares the wind profile measured in front of the empty turntable and the wind profile prescribed for category 0′ open sea terrain in Eurocode EN (1991)-1–4 (1991). The simulated ABL vertical wind velocity profile results agreed with the Eurocode $V_m(z)$ profile, with a +−10 % deviation.

Conf. 2 was placed on the centerline axis of the wind tunnel, and measurements were conducted under 0° wind direction. The WT was operated with a constant and unique wind speed. While independently using Irwin probes to measure PLW speeds (z=0.01 m), using a pitot tube, the reference wind speed (V_{ref}) at the reference location (z=0.01 m) was measured as 4.78 m/s and the turbulence intensity (I_v) as 0.15.

2.6. CFD implementation

The commercial CFD code STAR CCM+ was used to perform the simulations. CFD simulations were carried out on a reduced scale to save computational power without reducing accuracy (Ai & Mak, 2014) as we found no difference in the results between full-scale and reduced-scale runs. The computational domain of the CFD model has the same geometric dimensions as the wind tunnel. Therefore, the lateral and upper size of the computational domain corresponds to the wind tunnel size - 1.8 m × 2.5 m (height × width) in real scale. The inlet and

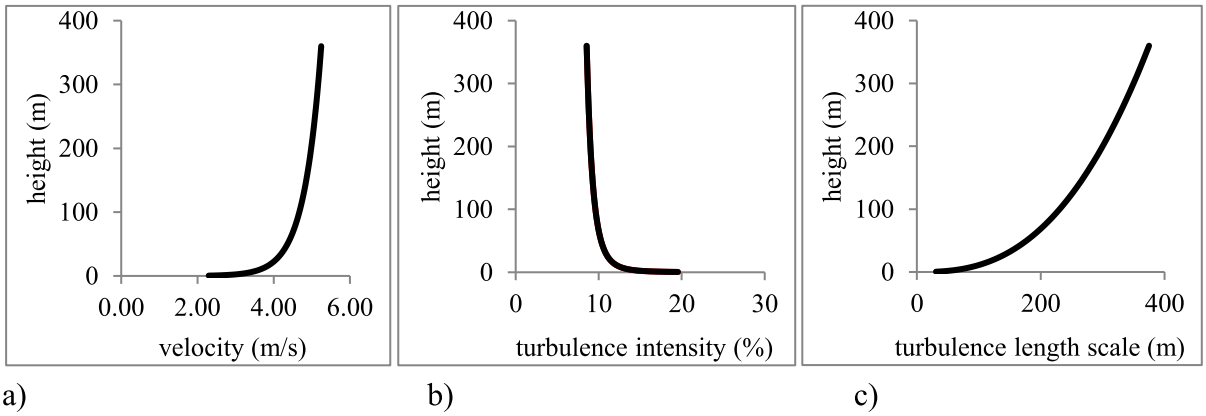

Fig. 10. Properties of the ABL vertical wind profile for category 0′ according to Eurocode EN (1991)-1-4 (1991) (a) mean velocity, (b) turbulence intensity, (c) turbulence length scale.

outflow computational boundaries were established as 5H and 15H, respectively (Franke et al., 2004), where H is the maximum building height. Accordingly, depending on seven different wind directions, the blockage ratio ranges from 2.43 to 4.78, 2.76 to 5.78, and 4 to 6.5 for Conf. 1, Conf. 2, and Conf. 3, respectively.

ABL vertical wind profile of category 0′, based on Eurocode EN (1991)-1–4 (1991), was specified as the inlet boundary condition. Fig. 10 illustrates the ABL wind profile properties (mean velocity, turbulence intensity, turbulence length scale).

The equivalent sand-grain roughness height (k_s) was calculated using Eq. (7) (Blocken et al., 2007), and to model the ground surface boundary conditions, Eq. (8) (Richards & Hoxey, 1993) was used:

$$ks = \frac{9.793 * z0}{Cs} \tag{7}$$

where the value 9.793 is the empirical wall constant E (–), z_0 is the aerodynamic roughness length, and c_s is the roughness constant (=1). Eq. (8) was utilised to ascertain the value of z_0, and k_s was found to be 1.4×10^{-3} m.

$$\frac{Uref}{u^*} = \frac{1}{\kappa}\ln\left(\frac{zref}{zo}\right) \tag{8}$$

where the von Karman constant (κ) is 0.41.

Slip / symmetrical wall boundary conditions were used on the lateral and upper boundaries, while no-slip and smooth wall boundary conditions were applied to building surfaces.

The issue of particle dispersion and wind gust analysis is out of the scope of this article. Thus, accurately predicting the mean wind speed is sufficient to meet the research objectives. Steady Reynolds-averaged Navier–Stokes (RANS) equations are widely utilised to estimate mean wind speed in PLW studies, whereas LES is ideal for resolving large eddies in a turbulent flow. However, the computation time needed to simulate large-scale configurations would be much greater (Zheng & Yang, 2021). Therefore, three-dimensional steady RANS equations were utilised to resolve the turbulent atmospheric boundary layer flow, and predict mean wind speed.

Reynolds Stress Model (RSM) model is widely used to evaluate average wind speeds around buildings in urban environments as it proves to be more effective than either standard k – ε or realisable k – ε models in predicting low-speed regions despite performing similarly in predicting high-speed regions (Reiter, 2010; Bas et al., 2023). Therefore, we used RSM to estimate the effect of turbulent fluctuation on the mean wind flow more accurately (Franke et al., 2007). The second-order upwind scheme was employed to discretise all transport equations, and the SIMPLE algorithm was used to couple the pressure and velocity

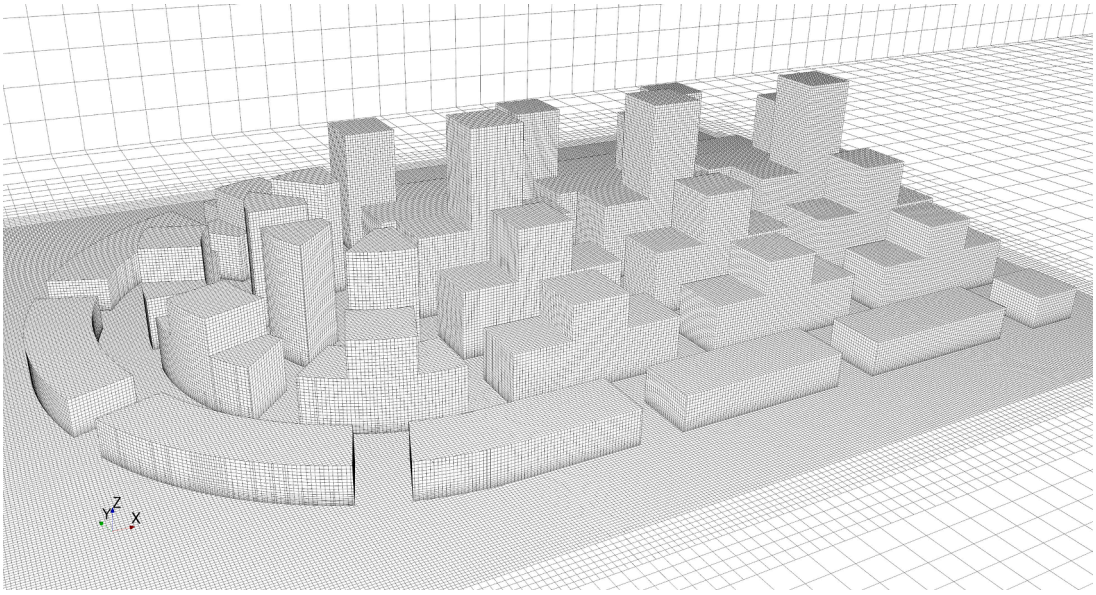

Fig. 11. View of the grid discretisation of Conf. 3 in the computational domain.

equations.

The computational domain was discretised with structured hexahedral elements (trimmed cell method), and ten prism layers with a stretching ratio of 1.2 were applied to near-wall boundaries to enhance accuracy (CD-Adapco, 2006). Fig. 11 shows the view of the grid discretisation in the computational domain of Conf. 3 with a 1 m grid cell size. The first layer thickness of the prism layer (y) from the ground was calculated by following the equations:

$$k = \frac{3}{2}(U(I)^2 \tag{9}$$

$$u^* = C_\mu^{1/4}\sqrt{k} \tag{10}$$

$$y = \frac{y^+ 2\nu}{u*} \tag{11}$$

where k is the turbulence kinetic energy (m^2/s^2), U (m/s) is the mean wind speed ($z_{ref} = 1m$), u^* is the ABL friction velocity (m/s), Cμ (=0.09) is the model constant, ν is the kinematic viscosity of air (m^2/s), y^+ is the dimensionless normal distance of the first cell centroids from the wall. By using these equations, when the desired y^+ was set to 30, the first layer thickness of the prism layer (y) was found to be 0.238 m according to the high Reynolds number ($30 < y^+ < 150$) wall function.

As a quality-control measure to reduce the spatial discretization error, the grid sensitivity test was conducted with grid cell sizes of 0.75 m (Grid 1), 1 m (Grid 2), and 1.5 m (Grid 3). We utilised the following equation to calculate the per cent error and to quantify the simulation accuracy of the three grid cell sizes: Percent error $= |(P(v) - M(v))/ M(v)| * 100\%$ where $P(v)$ is the wind velocity ratio calculated by CFD, and $M(v)$ is the measured wind velocity ratio in the wind tunnel experiment.

The per cent error for Grid 1, 2, and 3 was calculated to be 22.85 %, 23.5 %, and 36.5 %, respectively. The results demonstrate that Grid 1 and Grid 2 present similar results with an acceptable VR_w agreement, whereas Grid 3 is inadequate regarding simulation accuracy. However, Grid 1 is not computationally efficient as its simulation time is three times greater than Grid 2. Accordingly, the simulations were run using Grid 2.

A comparison of simulated and experimental wind velocity ratios (VR_w) of Conf. 2 at 2 m above the ground under 0° wind direction is demonstrated in Fig. 12. Overall, the CFD's predictive accuracy is in line with the experimental result. Nonetheless, the degree of accuracy differs in the high and low-velocity regions. The CFD model underestimates the wind velocity ratios at points 23–28, representing the low-velocity region behind buildings. This underestimation can be attributed to the limitations of RANS-type turbulence models, which tend to underestimate the low-velocity region (Zheng & Yang, 2021) while being relatively effective in predicting the high-velocity region. This indicates that the PLV efficiency may also be underestimated due to this limitation.

For urban aerodynamic studies that employ steady RANS turbulence models, a per cent error of up to 25 % is acceptable when assessing high-speed regions (Blocken et al., 2016). CFD validation yields satisfactory results with a per cent error of approximately 23.5 %, accounting for both high and low-speed areas at 0° wind direction.

As an additional quality control measure, scatter plots for each grid cell size were generated, as shown in Fig. 13 (a–c). The analysis reveals a positive linear correlation between the experiment and CFD results, as evidenced by the R-value of the three grid cell sizes, which exceeds 0.7. Grid 2 exhibits a robust positive correlation between the experiment and the CFD, with an R-value of 0.72.

3. Results

3.1. PLWE assessment

This section presents the evaluation of the PLW environment of the city configurations. The maximum VR_w values of the city configurations on coastal streets are shown in Fig. 14a. Considering the potential risk of PLW discomfort under seven wind directions in only coastal streets between the first-row blocks, the average maximum VR_w values are 1.34, 1.25, and 1.15 in Conf.1, Conf. 2, and Conf. 3, respectively. Fig. 14b shows city configurations' spatially averaged PLW comfort (SA_{PLWC}). Although SA_{PLWC} is >99 % in all configurations, it is lower in Conf. 1 than in Conf. 2 and Conf. 3. Our findings indicated that the grid street layout implemented in the coastal streets of Conf.1 led to a greater wind flow amplification (double corner effect) than the shifted street layout applied in Conf. 2 and Conf. 3. Although Conf. 2 and Conf. 3 have the same coastal street layout, VR_w never exceeds the maximum design wind speed threshold in Conf. 3. This is due to *adding a tower* on each second-row block (A2-B2). The added towers and the shifted street layout direct the wind behind the A1 and B2 arrays and reduce the wind amplification. A detailed explanation of this phenomenon will be given in the subsequent CFD analysis subsection.

Fig. 15(a-d) illustrates the maximum VR_w, SA_{PLWC}, SA_{PLVE}, and SA_{PLWE} of the designed configurations. When the results obtained from seven wind directions in all evaluation regions were evaluated, Conf. 2 and Conf. 3 displays a superior performance with an average maximum VR_w of 1,27 and 1.28, respectively, performing better than Conf.1 with an average maximum VR_w of 1.36 (Fig. 15a). The outcomes demonstrate that SA_{PLWC} was high in all configurations. In a negligible area (0–0.53 %), VR_w surpassed the maximum design wind speed threshold (VR_w=1.24) (Fig. 14b).

The SA_{PLVE} values in the evaluation region vary from 34 % to 73 %, with Conf. 2 achieving the highest SA_{PLVE} of 73 % under 0° wind direction. In this configuration, VR_w is higher than 0.34 (1 m/s) in 73 % of the evaluation region. Conf. 2 and Conf. 3 demonstrate similar outcomes and are better than Conf. 1. The reason for this is that the towers added to the city blocks have vastly enhanced SA_{PLVE} in Conf. 2 and Conf. 3. Generally, when the incidence angle of the wind rises from 0° to 90°, SA_{PLVE} decreases in both Conf. 2 and Conf. 3 similar to the findings of Ng (2009) and Qin et al. (2020), highlighting the positive effect of the

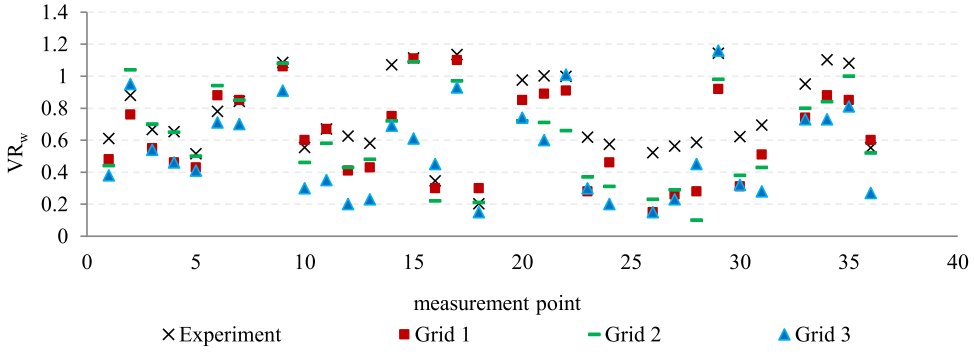

Fig. 12. Contrasting the wind velocity ratios (VR_w) between the experiment and three sizes of grid cells tested.

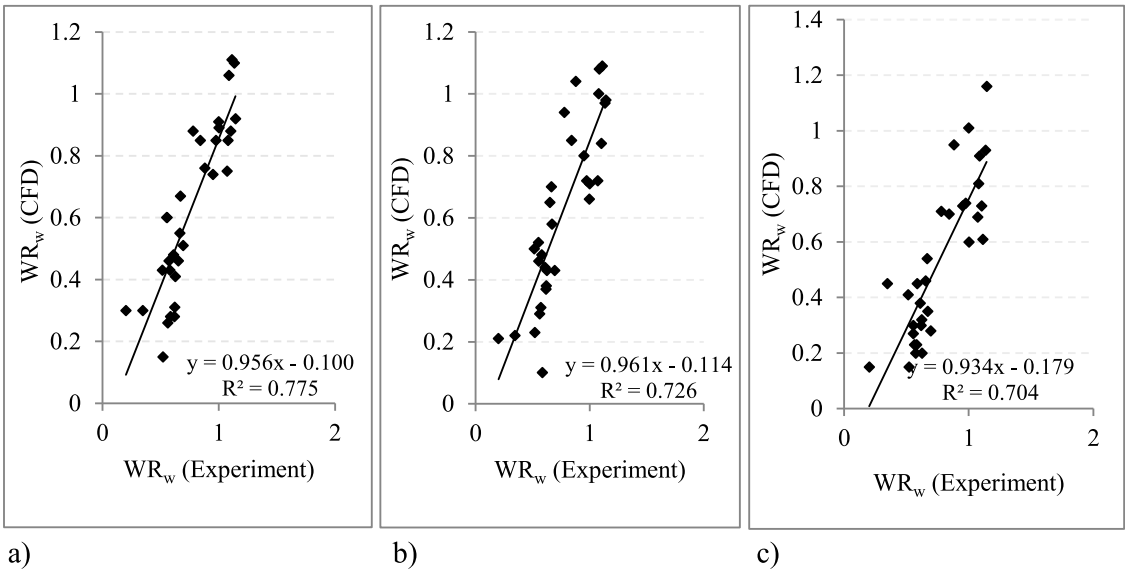

Fig. 13. Correlation of wind velocity ratios (WR_w) between the experiment and CFD, a) Grid 1, b) Grid 2, c) Grid 3.

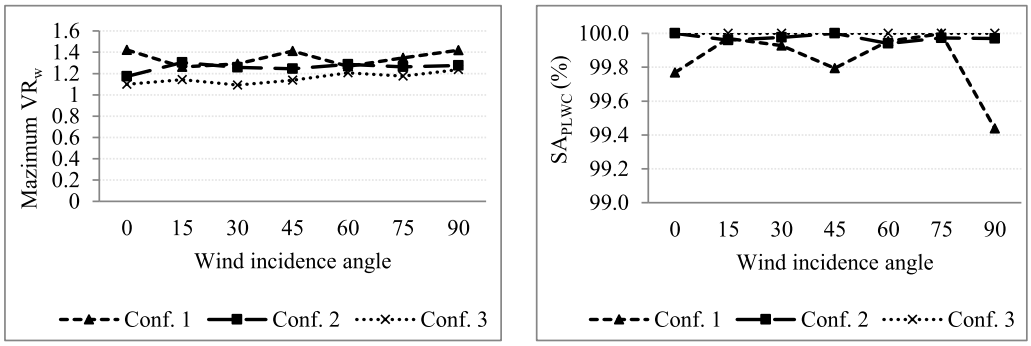

a) Maximum VR_w in coastal streets (z=2m) b) SA_{PLWC} in coastal streets (z=2m)

Fig. 14. Comparison of the maximum VR_w (a) and SA_{PLWC} (b) of the city configurations in coastal streets.

parallel orientation of the city blocks to the wind direction. Conf. 1 provides a better SA_{PLVE} performance between 30° and 75° wind incidence angles as these orientations lead to more coastal streets being exposed to the wind. A thorough explanation of this part will be given in the subsequent CFD analysis subsection.

Fig. 15d displays the SA_{PLWE} performance of the city configurations regarding both PLW comfort and PLV efficiency. The results indicate that Conf. 2 and Conf. 3 meet more target wind speed thresholds, and similar results were found for seven wind directions. According to this study's multi-performance objectives, the optimum city configuration is the one whose average SA_{PLWE} is the greatest while its average maximum VR_w is the least. We found that the average SA_{PLWE} for Conf.1, Conf. 2, and Conf. 3 is 48 %, 64 % and 62 %, respectively, and the average maximum VR_w for Conf. 1, Conf. 2, and Conf. 3 is 1.36, 1.28 and 1.27, respectively. Compared to other configurations, Conf. 2 creates a better PLW environment with a lower risk of PLW discomfort and higher PLV efficiency in the evaluation region, as indicated by the results for seven wind directions. However, the performance of Conf. 3 is relatively close to that of Conf. 2.

3.2. CFD analysis

Along with the general SA_{PLWE} appraisal, a more comprehensive PLW environment evaluation with a flow field visualization was carried out in this section. The results are depicted on contour plots with colours that denote different VR_w velocity ratios. Fig. 16 (a-j) displays the normalized velocity magnitude contour maps at pedestrian level (z=2 m) for 0° wind direction. The wind environments of (1) *weak* ($VR_w < 0.34$), (2) *strong* ($VR_w > 1.24$), and (3) *comfortable* $0.34 \leq VR_w \leq 1.24$ are categorized. The white blank spaces in Fig. 16 (a, d, and g) depict the areas whose VR_w values are below 1.24. Conversely, they indicate the areas with VR_w values above 0.34 in Fig. 16 (b, e, and h) and whose VR_w values are below 0.34 or above 1.24 in Fig. 16 (c, f, and j).

Fig. 16a, d, and g illustrate the position and size of the high-speed region. Despite the smallest blocks (H = 12 m) being used at A1 and B1 arrays, the *grid street layout* applied in Conf.1 increases wind flow around the street centre axis between upwind buildings. (Fig. 16a). The *shifted street layout* significantly reduces the wind flow amplification in coastal streets of Conf. 2 (Fig 16d) and Conf. 3 (Fig 16g). Nevertheless, it results in airflow stagnation between the B1–2, B2–2, and B2–3 blocks (Fig. 16e–h).

Adding towers to B2 arrays in Conf. 3 decreases wind amplification along the coastal streets (between B1–1 and B1–2, and B1–2 and B1–3) and enhances ventilation behind the B1–2 block better compared to Conf. 2. In Region A, the positive effect of *adding towers* to A3-A6 arrays on PLV efficiency is apparent in Conf. 2 and Conf. 3. Despite this, wind flow stagnation is especially noticeable behind the A5–1, A5–2, A6–1, and A6–2 rows in Conf. 3. This could be due to the towers in B2 and B3 rows obstructing the wind that would have reached region A in Conf. 3.

The wind is not directed along the coastal streets in Conf. 2 and Conf.

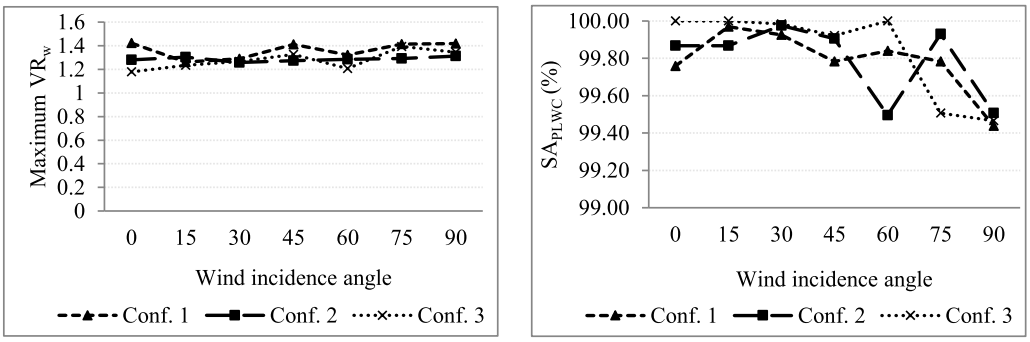

a) Maximum VR_w in the evaluation region (z=2m) b) SA_{PLWC} in the evaluation region (z=2m)

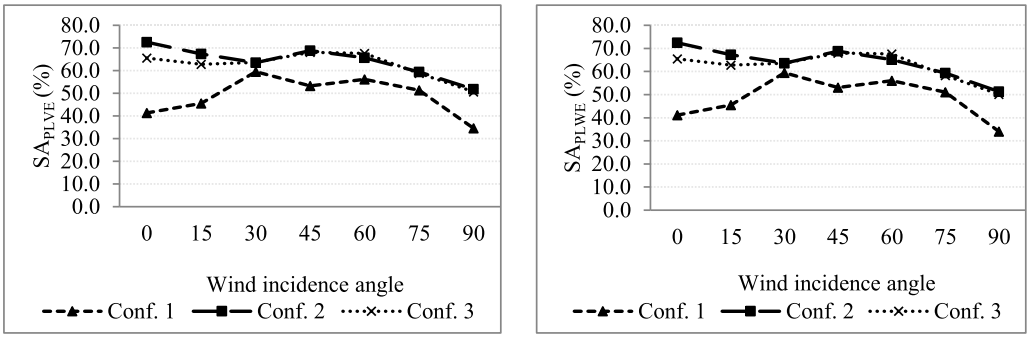

c) SA_{PLVE} in the evaluation region (z=2m) d) SA_{PLWE} in the evaluation region (z=2m)

Fig. 15. Comparison of the maximum VR_w a), SA_{PLWC} b), SA_{PLVE} c), and SA_{PLWE} d) of the city configurations in all evaluation regions.

3. Thus, the curved shape of the B2–2 and B2–3 blocks creates a powerful *channel effect* along the A2 and B2 arrays, respectively (Fig. 16f, j). A moderate *channel effect* is present in Conf.1 along the A4 array. The airflow divides in front of the A4–3 block and accelerates. Consequently, Conf. 2 is the most suitable to mitigate both strong and weak wind conditions of all the simulated configurations. Nevertheless, even Conf. 2 does not entirely impede wind stagnation.

Fig. 17(a–j) shows the contour plots of VR_w magnitudes for 90° wind direction at pedestrian level (z=2 m). Due to the grid street layout, a distinct wind amplification is observed on the coastal streets in Conf. 1 (Fig. 17a). *Shifted street layout* considerably diminishes wind amplification in Conf. 2 (Fig. 17d) and Conf. 3 (Fig. 17g). However, the *shifted street layout* and curved geometry of the B2 array generate an extensive wind corridor (channel effect) around the B2 array with the maximum VR_w reaching a value of 1.27.

When the wind direction is 90°, PLV efficiency is significantly diminished, resulting from the streets being perpendicular to the wind. The wind is most exposed to the longer sides of the blocks, which causes weaker wind areas in the streets behind them. Weak wind spreads over a much bigger area in Conf. 1 due to the absence of towers. The strategy of *adding towers* to A5-A6 arrays in the shifted layout is effective for averting weak wind areas in Conf. 2. By contrast, the strategy of *adding towers* to A2 arrays in Conf. 3 diminishes wind speed and generates vast zones of weak wind in the streets behind the A2 arrays.

Fig. 18(a–j) illustrates the contour plots of VR_w magnitudes at pedestrian level (z=2 m) for 45° wind direction. The positive effect of the *shifted street layout* in reducing wind amplification is observed in Conf. 2 (Fig. 18d) and Conf. 3 (Fig. 18g). Nevertheless, *adding towers* to the B2 arrays in Conf. 3 results in wind amplification around the B2–3 and B2–4 blocks.

Particularly noteworthy is that in Conf.1, PLV efficiency is better under 45° wind direction compared to 0° and 90° wind direction. Wind speed is above the minimum wind speed threshold in many regions. This is due to the more streets being exposed to oblique wind direction, similar to the findings of He et al. (2018) in their study of orthogonal breezeway networks (i.e., grid street) on pedestrian ventilation. However, under 45° wind direction, the weak wind problem behind the B1-B2 arrays persists in Conf. 2 and Conf. 3. Although many streets are well-ventilated, the city configurations are inadequate to ventilate the region behind the A6–1 and A6–2 blocks in the step-down street area.

3.2.1. *Analysis of wind flow patterns*

This section presents an analysis of the wind flow patterns, considering that wind direction can affect ventilation efficiency by changing pollutant dispersion characteristics and that circulation eddies can reduce the dispersion of pollutants to the upper layer. Fig. 19 (a-c) shows the normalized velocity magnitude vector maps between A1–2 and A1–3 row blocks for 90° wind direction at pedestrian level (z=2 m). A significant wind amplification (double-corner effect) is visible on the street between the first-row blocks in Conf. 1 due to the relatively *high-pressure difference* between the windward and leeward directions of the first-row blocks. The reason for the high-pressure difference is the rectangle-shaped buildings and grid street layout. In the grid street layout, the wind continues to flow along the street, and air mass is unable to adequately fill the negative pressure area behind the first row of blocks, causing weak wind speeds in the leeward region and wind amplification on the street center axis.

Compared to Conf. 1, the intensity of the *double-corner effect* was significantly reduced in Conf. 2. The reason for this is the shifted street layout, which directs the wind flow towards the leeward side of the first row blocks. Consequently, the leeward area gets filled with more air mass, and the pressure difference between the windward and leeward sides reduces, thus minimizing the intensity of the *double-corner effect* and increasing the wind velocity on the leeward side.

Similar to the shifted street layout strategy, *adding towers* to the second-row blocks in Conf. 3 allows wind to be directed to the leeward

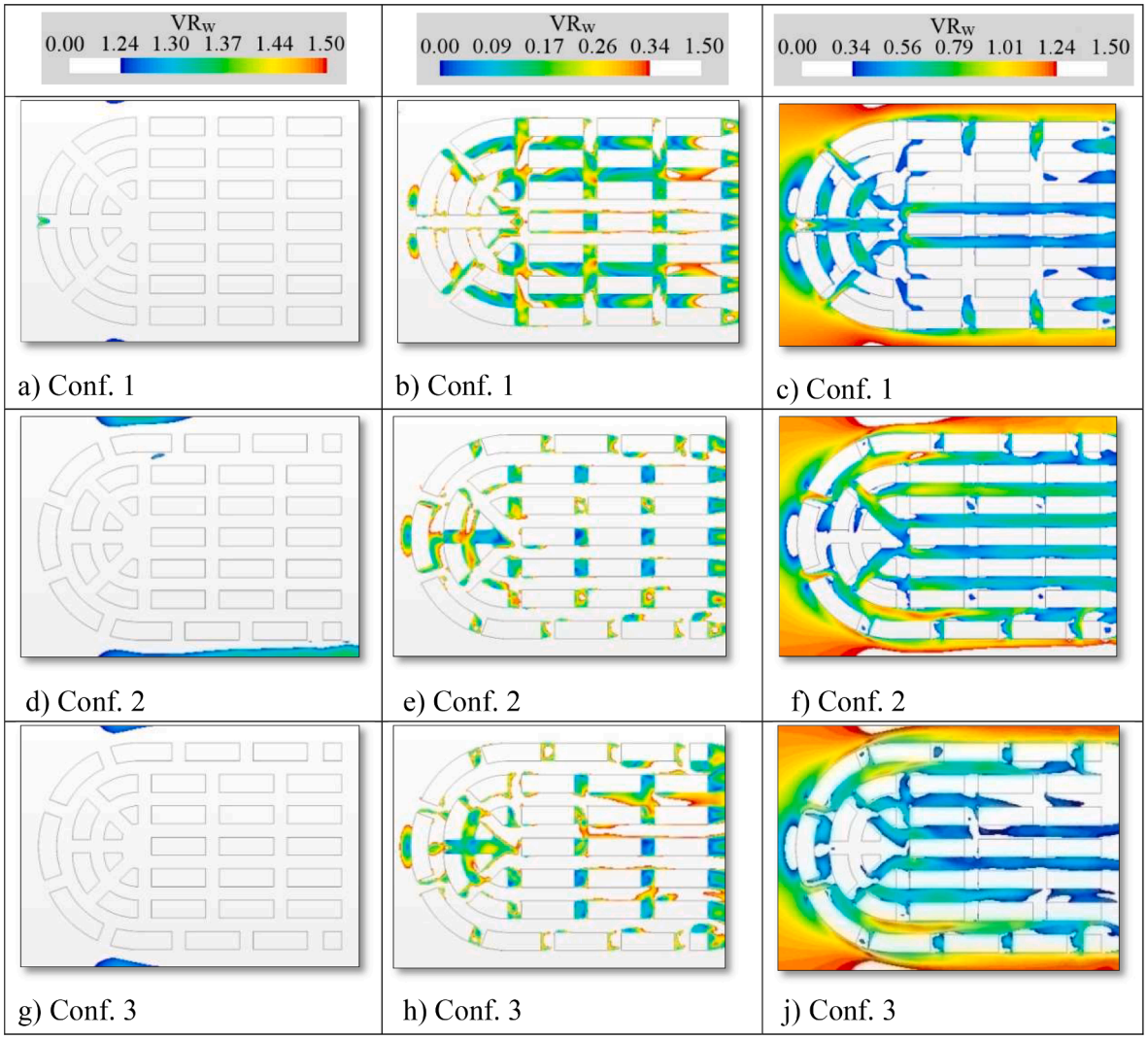

Fig. 16. Wind velocity ratio (VR_w) distribution under 0° (→) wind direction, a-ɒ-g) *strong* ($VR_w > 1.24$), b-e-h) *weak* ($VR_w < 0.34$), c-f-j) *comforTable* $0.34 \leq VR_w \leq 1.24$.

side of the first-row blocks. Therefore, the double corner effect is less pronounced in Conf. 3 than in Conf. 2, demonstrating that the combined efficacy of the strategies of *shifted street layout* and *adding towers* to the second-row blocks is greater. The *wind-directing effect* of these strategies is presented in Fig. 19. We found that the maximum VR_w behind the first-row of blocks is lowest in Conf. 1 with a maximum of 0.67 VR_w, moderate in Conf. 2 with a maximum of 0.97 VR_w, and highest in Conf. 3 with a maximum of 1.17 VR_w. In contrast, we found that the maximum VR_w on the coastal streets where the double corner effect occurs is highest in Conf. 1 with a maximum of 1.42 VR_w, moderate in Conf. 2 with a maximum of 1.27 VR_w, and lowest with a maximum of VR_w. 1.23 in Conf. 3. The findings indicate that *adding a tower* strategy to the second-row blocks can complement the *shifted street layout* strategy and provide better results in reducing the intensity of the double corner effect on coastal streets and increasing the ventilation behind the row blocks.

A wind flow pattern analysis was performed between the A1–2 and A7–2 blocks for 90° wind direction at pedestrian level (z=2 m), as shown in Fig. 20. This particular area was selected due to its relatively higher street aspect ratio and lower PLV efficiency. The result reveals significant differences in wind flow patterns between Conf. 1, Conf. 2, and Conf. 3 (Fig. 20a–c). Conf. 1 exhibits relatively stagnant wind flow, except for the coastal streets where the double corner effect is observed. Many low-speed circulatory vortexes are found in the leeward region behind the row blocks. In contrast, Conf. 2 and Conf. 3, which incorporate tower blocks, enhance wind velocity and have less vortex formation in the leeward region of row blocks. Our findings confirm the effectiveness of the applied strategy of arranging towers on the same axis in step-up blocks while adopting a shifted layout in step-down blocks.

It is noteworthy to mention that *adding towers* to second-row blocks in Conf. 3 significantly improves PLW comfort on coastal streets. However, this modification also contributes to the emergence of more stagnant wind conditions behind the second-row blocks than Conf. 2. Furthermore, not integrating towers into A7 blocks due to architectural concerns causes stagnant wind flow in front of the A7 blocks in all configurations.

A wind flow pattern analysis was performed between the A1–2 and A7–2 blocks at pedestrian level (z=2 m) in the longitudinal cross-section for 90° wind direction (Fig. 21). The section was taken from the central axis of the row blocks, including the coastal region and step-up and step-down street canyons with the towers. In Conf. 1, most areas at the pedestrian level are not ventilated efficiently except for the street canyon behind the first row blocks (A1). Despite implementing the step-up street canyon strategy, the majority of the wind tends to pass over the blocks, failing to reach the pedestrian level. In contrast, Conf. 2 exhibits well-ventilated areas at the pedestrian level. The *downwash effect* of the

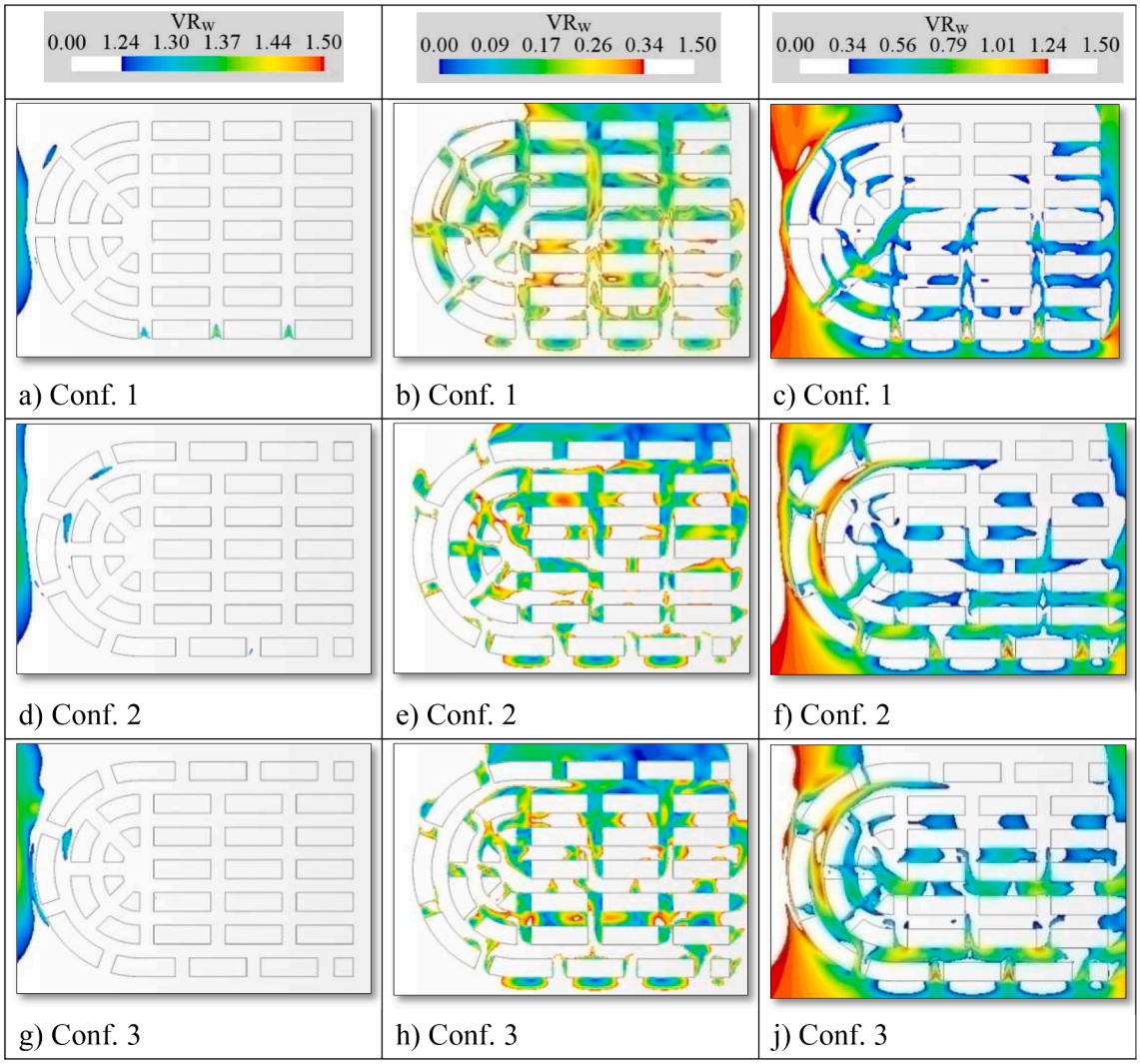

Fig. 17. Wind velocity ratio (VR_w) distribution under 90° (↑) wind direction, a-ᴅ-g) *strong* ($VR_w > 1.24$), b-e-h) *weak* ($VR_w < 0.34$), c-f-j) *comforTable* $0.34 \leq VR_w \leq 1.24$.

wind is particularly noticeable in front of the tower blocks. The towers separate the wind in front of it and divert relatively high-speed wind flow from a higher level to the ground level. This downward wind movement generates continuous and circulatory vortexes that generally dominate the wind flow pattern of the canyon. It is worth noting that the PLV efficiency in step-down street canyons is better than in Conf. 1. This is attributed to the positive effect of the shifted tower strategy on wind flow. Conf. 3 shows wind flow patterns similar to those of Conf. 2. However, weak wind regions behind the A2 block are present. This can be attributed to the tower added to the second-row array (A2), which obstructs wind from reaching the pedestrian level.

The results indicate that implementing a step-up street canyon with a 6 m block height increase, without the inclusion of towers, fails to enhance ventilation at the pedestrian level. The results also highlight the significance of relative positions and places of multiple towers in enhancing ventilation. In this integrated approach, buildings play a pivotal role in directing top wind to the pedestrian level by acting as wind catchers rather than obstructing the wind flow.

4. Discussion

This study presented the design of three city configurations to improve the PLW environment. Although most of the multi-performance objectives of the study were satisfied, conflicting results require discussion.

4.1. Role of street layout and adding towers on wind comfort

Several studies focused on improving pedestrian wind comfort in coastal cities exposed to open wind conditions. In agreement with our findings, Bas et al. (2022) proposed to apply a shifted street layout using relatively narrow streets (4–10 m), small building widths (20 m), and moderate building heights (25 m); thus, they provided a maximum VR_w between 1.0 and 1.05 in coastal streets only under the perpendicular wind direction. Unlike the previous study, wider building widths (60 m) and towers (66 m) were used, focusing on the future development of Cape Punta. As a result, an average maximum VR_w of 1.25 was attained on coastal streets under seven different wind directions, indicating the influence of different building sizes on the results.

In Conf. 3, a well-known building-building interaction was created consisting of a low-rise building in the first row and a tower in the second row. Such an interaction could have resulted in a strong downwash effect in the canyon in front of it (Stathopoulos, 2009). However, since the height of the tower in the second-row blocks was only 12 m higher than the height of the first-row blocks, and the span between the first and second-row blocks was quite wide (15 m), the wind amplification was limited.

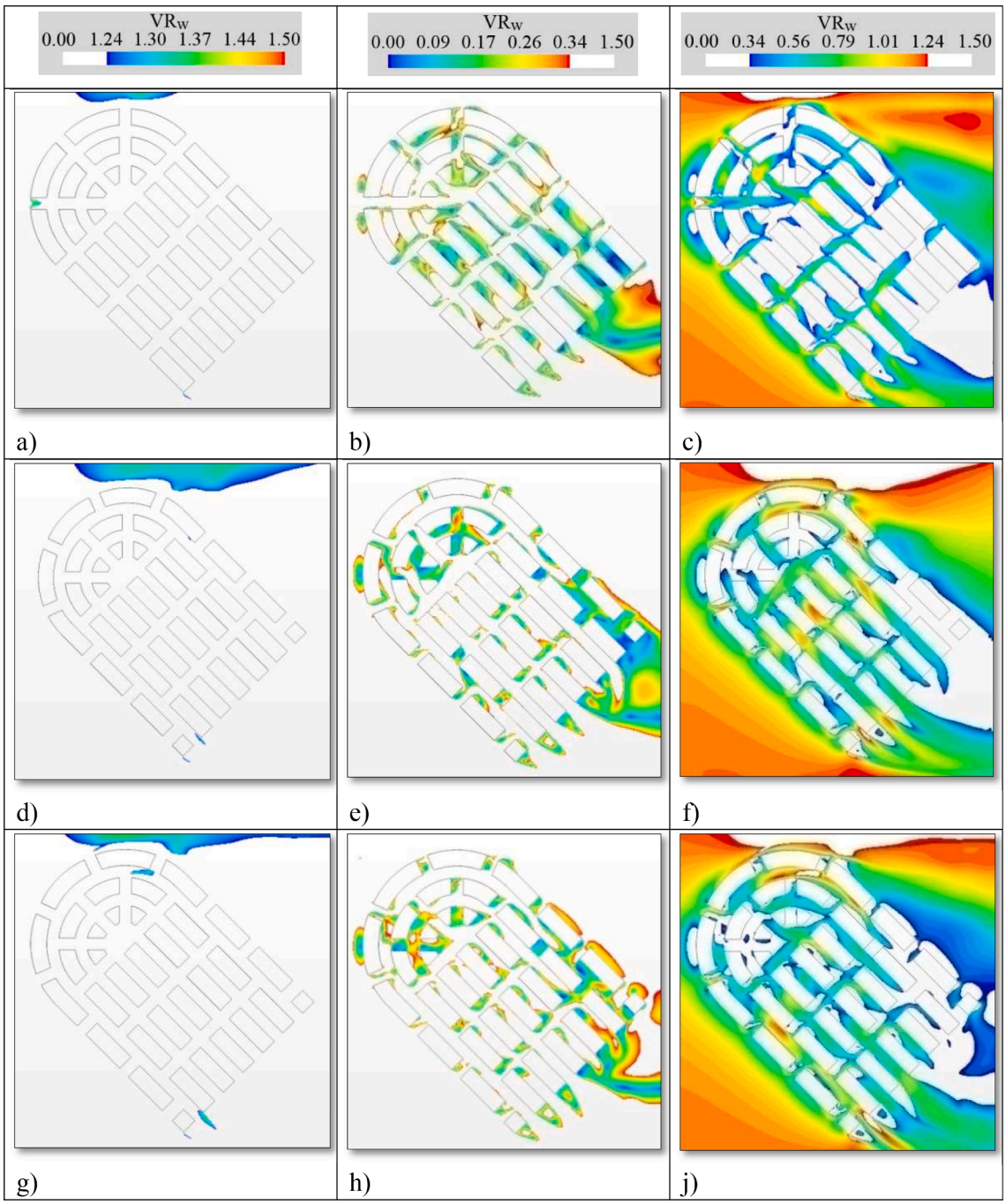

Fig. 18. Wind velocity ratio (VR_w) distribution under 45° (↘) wind direction, a-ɒ-g) *strong* ($VR_w > 1.24$), b-e-h) *weak* ($VR_w < 0.34$), c-f-j) *comforTable* $0.34 \leq VR_w \leq 1.24$.

4.2. Role of street canyon form and adding towers on outdoor ventilation

Numerous studies confirmed that step-up street canyons enhance ventilation more than even and step-down canyons (Chew et al., 2017; Xu et al., 2023; Pan & Ji, 2024). Our findings verified that PLV efficiency in the step-down canyons is generally lower than in the step-up canyons. Unlike the earlier study, this study also demonstrated how to boost weak winds in step-down canyons with a shifted tower layout applied on A5 and A6 arrays.

According to the studies conducted by Tsang et al. (2012) and Hang et al. (2012), shorter building widths are better for outdoor ventilation. Similar to previous findings, Conf. 1 revealed the negative impact of row buildings with larger widths on outdoor ventilation. In contrast, the city configurations with towers significantly reduced the negative impact of row buildings.

4.3. Applicability of findings to other climatic regions

The Mediterranean climate and site-specific context of Cape Punta require equal consideration of outdoor ventilation and wind comfort. While Conf. 2 is better than Conf. 3 for outdoor ventilation, Conf. 3 is better than Conf. 2 in preventing wind discomfort risk in coastal streets. Therefore, the strategies applied in Conf. 3 could be used in climates where coastal streets have stronger wind speeds than Cape Punta, and pedestrian wind comfort is more important than outdoor ventilation. Conversely, in climates where outdoor ventilation is a priority,

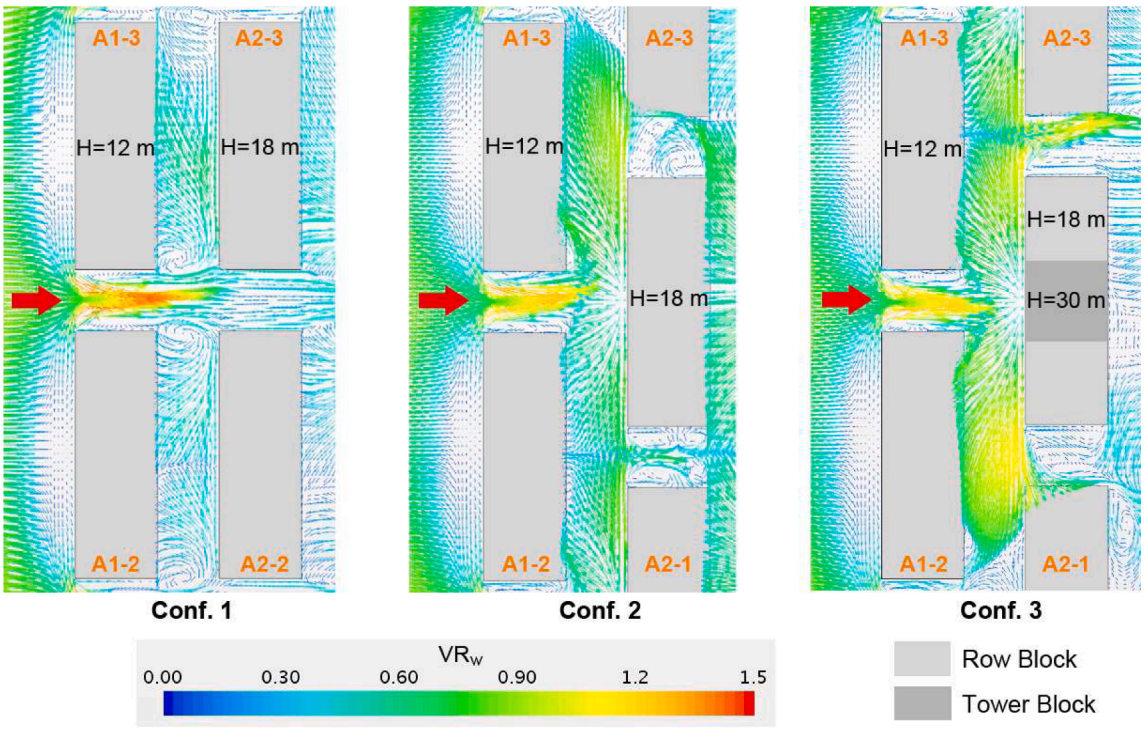

Fig. 19. Normalized velocity magnitude vector map between A1 and A2 block arrays for 90° wind direction at pedestrian level (z=2 m).

ventilation can be improved by increasing the towers' height and implementing the grid street layout strategy. However, in each climatic region, the climate-based minimum and maximum wind speed thresholds must be readjusted, and site-specific tests must be conducted. In this regard, this study provides a flexible selection framework considering the climatic dissimilarities.

4.4. Limitations

The study's main limitation is that the seasonal variability of the desired wind thresholds is not considered. The simulations were conducted under conditions of constant annual mean wind speed; however, in summer, the average speed of the sea breeze increases, which means that more positive results regarding reducing UHI and air pollution will occur in the summer months, and more negative effects will occur in the winter months. However, given that extreme temperatures in summer cause thermal stress on local populations and take precedence over the risk of wind discomfort and air quality, it is possible to ignore this limitation. In this regard, the present study is a first step towards an even more integrated and multi-disciplinary study that will consider seasonal variability of the desired wind thresholds based on local temperature data in the future.

This study focused on taking advantage of the sea breeze since it positively affects the city's ventilation more than other winds. On the other hand, since large city configurations require a high amount of simulation computation time, only seven wind directions were considered. Although this hypothetical approach enables the design of more reactive city configurations adapted to the sea breeze, the lack of statistical analysis of the different wind directions is another limitation.

The other limitation of this study is the turbulence model (RSM), which underestimates the mean wind speed in low-speed regions compared to wind tunnel results. Considering this limitation, PLV efficiency could be higher, resulting in better ventilation prediction outcomes. LES could be superior (Zheng & Yang, 2021), yet the computational time required to simulate large-scale city configurations is still much longer.

4.5. Future perspectives

Further research will be conducted on the optimal size and placement of towers on city blocks. Moreover, further research will evaluate designing new techniques to eliminate weak wind in step-down street canyons. On the other hand, further research will focus on developing city configurations adapted to more wind directions based on a statistical examination of pedestrian wind comfort. In this regard, seasonal thresholds will be studied to consider more accurately the influence of wind on thermal comfort and UHI, in addition to its impact on wind comfort and urban ventilation.

5. Conclusions

Pedestrian wind comfort and outdoor ventilation are crucial for increasing the livability and comfort of Mediterranean cities. However, they have contradictory requirements regarding wind speeds in urban planning. This study presented a multi-purposed design of city configurations to optimise pedestrian-level ventilation and wind comfort requirements in the Mediterranean compact coastal city context. CFD simulations were conducted to examine the combined effect of a set of urban morphological strategies on the PLW environment. The findings demonstrate that although weak wind flow is not entirely prevented in the step-down street canyons, a compromise between PLW comfort and PLV efficiency requirements is achieved. Six key findings should be emphasised:

- The shifted coastal street layout directs the wind toward the leeward side of the first-row blocks and reduces the pressure difference between the windward and leeward sides. Thus, it reduces the intensity of the double corner effect by 10 % compared to a grid coastal street layout.
- Adding towers to the second-row blocks integrated with the shifted coastal street layout directs the wind toward the leeward side of the first-row blocks similarly and reduces the intensity of the double corner effect by 20 % compared to a grid coastal street layout.

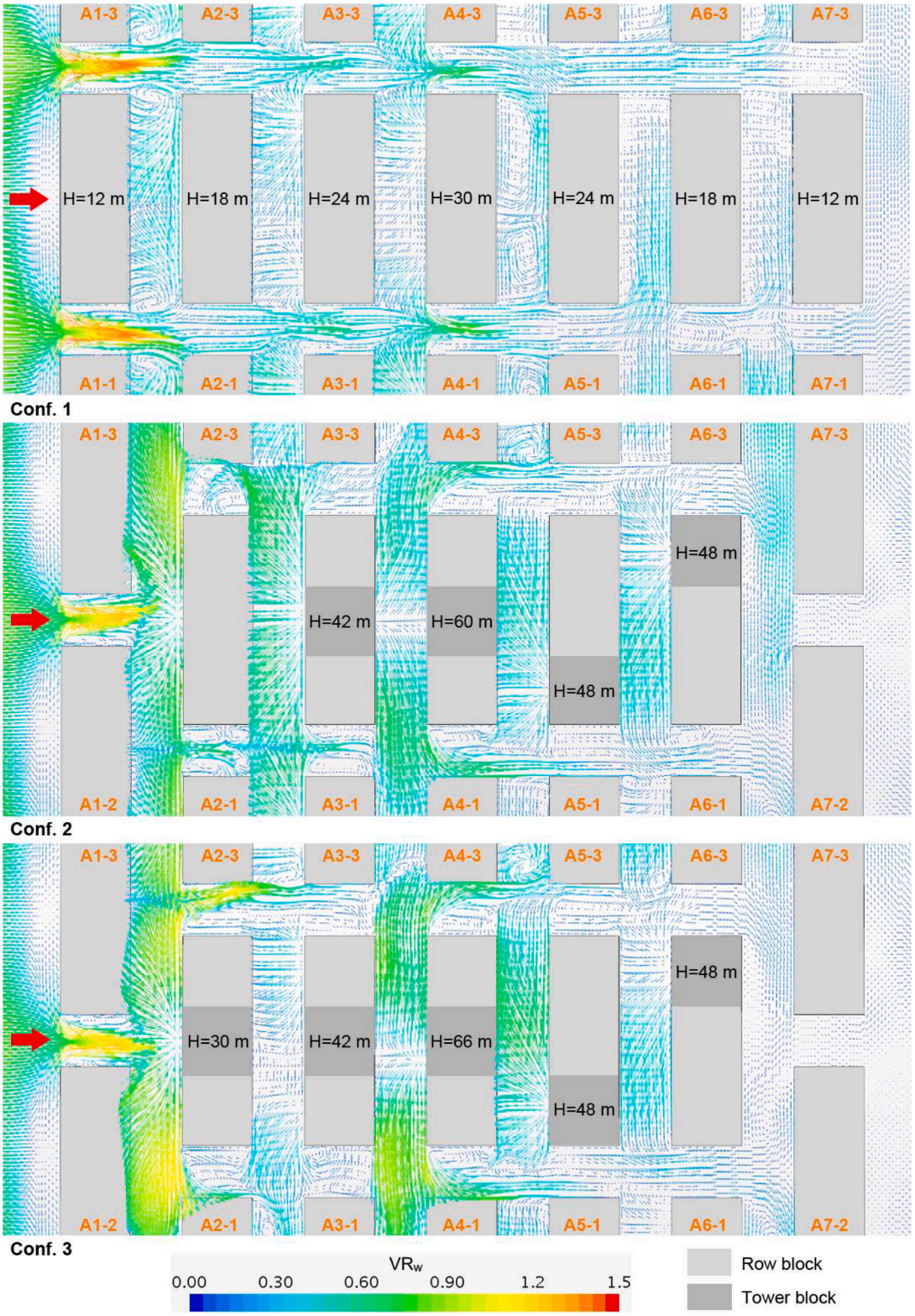

Fig. 20. Normalized velocity magnitude vector map between A1 and A7 block arrays for 90° wind direction at pedestrian level (z=2 m).

- Combining step-up and step-down street canyons with a block height difference of 6 m can increase the PLW efficiency by up to 41 %. However, positioning step-up towers on step-up row blocks and shifted towers on step-down row blocks can increase PLW efficiency by up to 73 %, highlighting the crucial role of relatively positioned multiple towers in enhancing ventilation.
- Ventilation performance is mostly affected by the orientation of the streets. Keeping row blocks oriented parallel to the prevailing wind enhances PLW efficiency.
- In Conf.1, a remarkable increase in SA_{PLVE} is observed as there are more coastal streets that draw wind into street canyons when the wind is blowing obliquely.

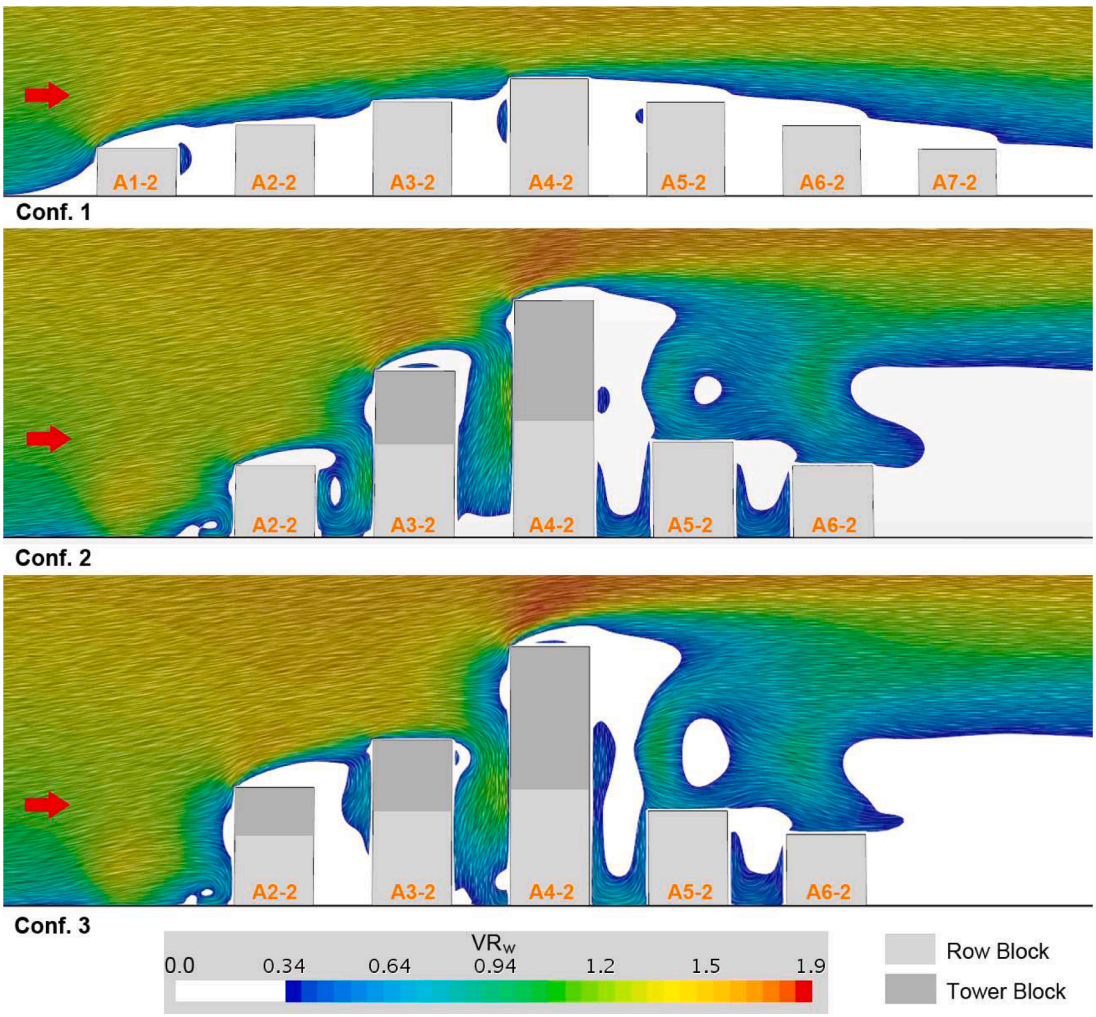

Fig. 21. Normalized velocity magnitude vector map between A1 and A7 block arrays in the longitudinal cross-section for a wind direction of 90°.

- The curved geometry of city blocks in Region B creates a channel effect, increasing PLW speed.

The findings demonstrate that the cumulative effect of multiple strategies yields more significant improvements in mitigating strong and weak wind problems. Based on the findings, this study provides extensive scientific findings and practical implications to benefit numerous stakeholders. First, architects and urban planners can use the findings to improve PLV efficiency and PLW comfort in urban areas. Second, urban policymakers can benefit from this study when planning the future design and site-specific wind planning of Cape Punta. Finally, the findings support today's sustainable and compact city concept, as the more compact configurations (Conf. 2 and Conf. 3) demonstrate better outdoor ventilation and wind comfort results.

The findings can be employed in other cities with similar climates in new development, expansion, and renovation. Enhancing PLV efficiency and PLW comfort can promote pedestrian activities, urban walkability, cyclability, and the livability of urban habitats. The research methodology based on defining wind speed thresholds adapted to local wind characteristics and using a multi-objective optimisation can be transferred to other climates and urban environments to produce findings adapted to these contexts.

Based on the findings, the authors propose a multi-purpose, holistic, and large-scale study approach to mitigate wind-related urban environmental problems beyond Mediterranean cities. Furthermore, as shown in this study, building height variation is an effective geometric indicator to simultaneously improve wind comfort and ventilation. However, in many cities, pre-determined building height limits hinder the benefits of building height variation. Therefore, the authors propose that more flexible building and zoning regulations be applied in planning new settlements, particularly in warm climates or regions with strong wind climates. Although it is not easy to achieve a universal hypothetical optimized urban form that meets these recommendations and is valid in all climatic regions, in these conditions, architects can design more reactive and optimized urban forms to improve the PLW environment. In this regard, the methodology developed in this study may be helpful.

Funding

This work was supported by the Local Environmental Management and Analysis (LEMA) Unit in the Applied Sciences Faculty of the University of Liège and the Scientific and Technological Research Council of Turkiye (TUBITAK) under the Grant number 123M733. The authors thank LEMA and TUBITAK for their support. The authors also thank the anonymous reviewers for their valuable comments that improve the study.

CRediT authorship contribution statement

Hakan Baş: Writing – original draft, Visualization, Validation, Software, Resources, Project administration, Methodology,

Investigation, Funding acquisition, Formal analysis, Data curation, Conceptualization. **Thomas Andrianne:** Writing – review & editing, Validation, Supervision, Resources, Methodology, Investigation, Conceptualization. **Sigrid Reiter:** Writing – review & editing, Supervision, Resources, Methodology, Funding acquisition, Conceptualization.

Declaration of competing interest

The authors declare the following financial interests/personal relationships which may be considered as potential competing interests:

Sigrid Reiter reports financial support was provided by University of Liege. Hakan Bas reports financial support was provided by Scientific and Technological Research Council of Turkey. If there are other authors, they declare that they have no known competing financial interests or personal relationships that could have appeared to influence the work reported in this paper.

Data availability

Data will be made available on request.

References

Ai, Z. T., & Mak, C. M. (2014). Potential use of reduced-scale models in CFD simulations to save numerical resources: Theoretical analysis and case study of flow around an isolated building. *Journal of Wind Engineering and Industrial Aerodynamics, 134*, 25–29.

Allegrini, J., Dorer, V., & Carmeliet, J. (2015). Coupled CFD, radiation and building energy model for studying heat fluxes in an urban environment with generic building configurations. *Sustainable Cities and Society, 19*, 385–394.

Arkon, C. A., & Özkol, Ü. (2014). Effect of urban geometry on pedestrian-level wind velocity. *Architectural Science Review, 57*(1), 4–19.

Baik, J. J., & Kim, J. J. (1999). A numerical study of flow and pollutant dispersion characteristics in urban street canyons. *Journal of Applied Meteorology and Climatology, 38*(11), 1576–1589.

Baş, H., Dogrusoy, I. T., & Reiter, S. (2022). Wind adaptive urban seafront buildings design for improving urban ventilation and pedestrian wind comfort in Mediterranean climate. *International Journal of Global Warming, 28*(3), 239–259.

Baş, H., Doğrusoy, I. T., & Reiter, S. (2023). A proposal of urban coastal pattern for improving pedestrian wind comfort in coastal cities. *Journal of Building Physics, 47*(2), 151–181.

Blocken, B., Stathopoulos, T., & Carmeliet, J. (2007). CFD simulation of the atmospheric boundary layer: Wall function problems. *Atmospheric Environment, 41*(2), 238–252.

Blocken, B., Stathopoulos, T., & Van Beeck, J. P. A. J. (2016). Pedestrian-level wind conditions around buildings: Review of wind-tunnel and CFD techniques and their accuracy for wind comfort assessment. *Building and Environment, 100*, 50–81.

Buccolieri, R., Sandberg, M., & Di Sabatino, S. (2010). City breathability and its link to pollutant concentration distribution within urban-like geometries. *Atmospheric Environment, 44*(15), 1894–1903.

Anon CD-Adapco, 2006. Star-CCM+ version 4.02.011 user guide. London, UK.

Chen, L., Hang, J., Sandberg, M., Claesson, L., Di Sabatino, S., & Wigo, H. (2017). The impacts of building height variations and building packing densities on flow adjustment and city breathability in idealized urban models. *Building and Environment, 118*, 344–361.

Chen, G., Rong, L., & Zhang, G. (2021). Impacts of urban geometry on outdoor ventilation within idealized building arrays under unsteady diurnal cycles in summer. *Building and Environment, 206*, Article 108344.

Chew, L. W., Nazarian, N., & Norford, L. (2017). Pedestrian-level urban wind flow enhancement with wind catchers. *Atmosphere, 8*(9), 159.

Chohan, A. H., & Awad, J. (2022). Wind catchers: An element of passive ventilation in hot, arid and humid regions, a comparative analysis of their design and function. *Sustainability, 14*(17), 11088.

Coccia, M. (2020). How (un) sustainable environments are related to the diffusion of COVID-19: The relation between coronavirus disease 2019, air pollution, wind resource and energy. *Sustainability, 12*(22), 9709.

Anon Eurocode, EN 1991-1-4. (1991). Actions on structures-general actions-wind actions. *European Committee for Standardization*.

Franke, J., Hirsch, Ch., Jensen, A. G., Krüs, H. W., Schatzmann, M., Westbury, P. S., & Wright, N. G. (2004). *Recommendations on the use of cfd in predicting pedestrian wind environment, 14*. Cost action C.

Franke, J., Hellsten, A., Schlünzen, H., & Carissimo, B. (2007). *Best practice guideline for the cfd simulation of flows in the urban environment. cost action 732. quality assurance and improvement of meteorological models*. University of Hamburg, Meteorological Institute, Center of Marine and Atmospheric Sciences.

Gu, Z. L., Zhang, Y. W., Cheng, Y., & Lee, S. C. (2011). Effect of uneven building layout on air flow and pollutant dispersion in non-uniform street canyons. *Building and Environment, 46*(12), 2657–2665.

Gu, K., Fang, Y., Qian, Z., Sun, Z., & Wang, A. (2020). Spatial planning for urban ventilation corridors by urban climatology. *Ecosystem Health and Sustainability, 6*(1), Article 1747946.

Guo, A., Yue, W., Yang, J., Li, M., Xie, P., He, T., & Yu, H. (2023). Quantifying the impact of urban ventilation corridors on thermal environment in Chinese megacities. *Ecological Indicators, 156*, Article 111072.

Hang, J., Li, Y., Buccolieri, R., Sandberg, M., & Di Sabatino, S. (2012). On the contribution of mean flow and turbulence to city breathability: The case of long streets with tall buildings. *The Science of the Total Environment, 416*, 362–373.

Hang, J., Wang, Q., Chen, X., Sandberg, M., Zhu, W., Buccolieri, R., & Di Sabatino, S. (2015). City breathability in medium density urban-like geometries evaluated through the pollutant transport rate and the net escape velocity. *Building and Environment, 94*, 166–182.

He, Y., Tablada, A., & Wong, N. H. (2018). Effects of non-uniform and orthogonal breezeway networks on pedestrian ventilation in Singapore's high-density urban environments. *Urban Climate, 24*, 460–484.

He, B. J., Ding, L., & Prasad, D. (2019). Enhancing urban ventilation performance through the development of precinct ventilation zones: A case study based on the Greater Sydney, Australia. *Sustainable Cities and Society, 47*, Article 101472.

He, B. J., Ding, L., & Prasad, D. (2020). Relationships among local-scale urban morphology, urban ventilation, urban heat island and outdoor thermal comfort under sea breeze influence. *Sustainable Cities and Society, 60*, Article 102289.

Hu, T., & Yoshie, R. (2013). Indices to evaluate ventilation efficiency in newly-built urban area at pedestrian level. *Journal of Wind Engineering and Industrial Aerodynamics, 112*, 39–51.

Huang, Y., Hu, X., & Zeng, N. (2009). Impact of wedge-shaped roofs on airflow and pollutant dispersion inside urban street canyons. *Building and Environment, 44*(12), 2335–2347.

Ignatius, M., Wong, N. H., & Jusuf, S. K. (2015). Urban microclimate analysis with consideration of local ambient temperature, external heat gain, urban ventilation, and outdoor thermal comfort in the tropics. *Sustainable Cities and Society, 19*, 121–135.

Irwin, H. P. A. H. (1981). A simple omnidirectional sensor for wind-tunnel studies of pedestrian-level winds. *Journal of Wind Engineering and Industrial Aerodynamics, 7*(3), 219–239.

Isyumov, N., & Davenport, A. G. (1975). The ground level wind environment in built-up areas. In *Proceedings of the 4th international conference on wind effects on buildings and structures* (pp. 403–422). . Heathrow.

Anon İzmirMag, 2016. Dünden Bugüne Kordon'un Geçirdiği Evrimin Hikayesi. https://izmirmag.net/dunden-bugune-kordonun-gecirdigi-evrimin-hikayesi/. (accessed 13 September 2023).

Johansson, E., & Yahia, M. W. (2020). *Wind comfort and solar access in a coastal development in malmö, 33*. Sweden. Urban Clim, Article 100645.

Kato, S., & Hiyama, K. (2012). *Ventilating cities: Air-flow criteria for healthy and comfortable urban living*. Springer Science & Business Media.

Montazeri, H. (2011). Experimental and numerical study on natural ventilation performance of various multi-opening wind catchers. *Building and Environment, 46*(2), 370–378.

Mouratidis, K. (2019). Compact city, urban sprawl, and subjective well-being. *Cities, 92*, 261–272 (London, England).

Ng, E. (2009). Policies and technical guidelines for urban planning of high-density cities–air ventilation assessment (AVA) of Hong Kong. *Building and Environment, 44*(7), 1478–1488.

Oh, M., & Kim, Y. (2019). Identifying urban geometric types as energy performance patterns. *Energy for Sustainable Development, 48*, 115–129.

Orosa, J. A., Kameni Nematchoua, M., & Reiter, S. (2020). Air changes for healthy indoor ambiences under pandemic conditions and its energetic implications: A Galician case study. *Applied Sciences, 10*(20), 7169.

Palusci, O., Monti, P., Cecere, C., Montazeri, H., & Blocken, B. (2022). Impact of morphological parameters on urban ventilation in compact cities: The case of the Tuscolano-Don Bosco district in Rome. *The Science of the Total Environment, 807*, Article 150490.

Pan, J., & Ji, J. (2024). Influence of building height variation on air pollution dispersion in different wind directions: A numerical simulation study. *Applied Sciences, 14*(3), 979.

Qin, H., Lin, P., Lau, S. S. Y., & Song, D. (2020). Influence of site and tower types on urban natural ventilation performance in high-rise high-density urban environment. *Building and Environment, 179*, Article 106960.

Reiter, S. (2010). Assessing wind comfort in urban planning. *Environment and Planning B Planning and Design, 37*(5), 857–873.

Richards, P. J., & Hoxey, R. P. (1993). Appropriate boundary conditions for computational wind engineering models using the k-ϵ turbulence model. *Journal of Wind Engineering and Industrial Aerodynamics, 46*, 145–153.

Shirzadi, M., Tominaga, Y., & Mirzaei, P. A. (2020). Experimental and steady-RANS CFD modelling of cross-ventilation in moderately-dense urban areas. *Sustainable Cities and Society, 52*, Article 101849.

Stathopoulos, T., & Wu, H. (1995). Generic models for pedestrian-level winds in built-up regions. *Journal of Wind Engineering and Industrial Aerodynamics, 54*, 515–525.

Stathopoulos, T. (2009). Wind and comfort. In *Proceedings of the 5th European and African conference on wind engineering* (pp. 67–82).

Stewart, I. D., & Oke, T. R. (2012). Local climate zones for urban temperature studies. *Bulletin of the American Meteorological Society, 93*(12), 1879–1900. https://doi.org/10.1175/BAMS-D-11-00019.1

Tsang, C. W., Kwok, K. C. S., & Hitchcock, P. A. (2012). Wind tunnel study of pedestrian level wind environment around tall buildings: Effects of building dimensions, separation and podium. *Building and Environment, 49*, 167–181.

Anon. Turkish State Meteorological Service [T.S.M.S.], 2024 Climate data, Türkiye.
Vita, G., Shu, Z., Jesson, M., Quinn, A., Hemida, H., Sterling, M., & Baker, C. (2020). On the assessment of pedestrian distress in urban winds. *Journal of Wind Engineering and Industrial Aerodynamics, 203*, Article 104200.
Voogt, J. A. (2004). *Urban heat islands: Hotter cities*. America Institute of Biological Sciences.
Wang, W., Wang, D., Chen, H., Wang, B., & Chen, X. (2022). Identifying urban ventilation corridors through quantitative analysis of ventilation potential and wind characteristics. *Building and Environment, 214*, Article 108943.
Xie, X., Huang, Z., Wang, J., & Xie, Z. (2005). The impact of solar radiation and street layout on pollutant dispersion in street canyon. *Building and Environment, 40*(2), 201–212.
Xie, P., Yang, J., Wang, H., Liu, Y., & Liu, Y. (2020). A New method of simulating urban ventilation corridors using circuit theory. *Sustainable Cities and Society, 59*, Article 102162.
Xie, P., Yang, J., Sun, W., Xiao, X., & Xia, J. C. (2022). Urban scale ventilation analysis based on neighborhood normalized current model. *Sustainable Cities and Society, 80*, Article 103746.
Xu, Q., & Xu, Z. (2020). What can urban design learn from changing winds? A case study of public space in Nanjing (1990s-2010s). *Journal of Public Space, 5*(2), 7–22.
Xu, W., Zhao, L., Zhang, Y., & Gu, Z. (2023). Investigation on air ventilation within idealised urban wind corridors and the influence of structural factors with numerical simulations. *Sustainability, 15*(18), 13817.
Zhang, X., Estoque, R. C., & Murayama, Y. (2017). An urban heat island study in Nanchang City, China based on land surface temperature and social-ecological variables. *Sustainable Cities and Society, 32*, 557–568.
Zhao, Z., Shen, L., Li, L., Wang, H., & He, B. J. (2020). Local climate zone classification scheme can also indicate local-scale urban ventilation performance: An evidence-based study. *Atmosphere, 11*(8), 776.
Zheng, X., & Yang, J. (2021). CFD simulations of wind flow and pollutant dispersion in a street canyon with traffic flow: Comparison between RANS and LES. *Sustainable Cities and Society, 75*, Article 103307.